Review

Fault Detection of Permanent Magnet Synchronous Machines: An Overview

Henghui Li , Z.Q. Zhu * , Ziad Azar , Richard Clark , Zhanyuan Wu

Posted Date: 24 December 2024

doi: 10.20944/preprints202412.1988.v1

Keywords: demagnetization; eccentricity; fault detection; fault signature; inter-turn short-circuit; permanent magnet; permanent magnet synchronous machine

Review

Fault Detection of Permanent Magnet Synchronous Machines: An Overview

Henghui Li [1], Z.Q. Zhu [1,*], Ziad Azar [2], Richard Clark [2] and Zhanyuan Wu [2]

[1] School of Electrical and Electronic Engineering, University of Sheffield, Mappin Street, Sheffield S1 3JD, UK; hli214@sheffield.ac.uk (H.L.); z.q.zhu@sheffield.ac.uk (Z.Q.Z.)
[2] Sheffield Siemens Gamesa Renewable Energy Research Centre, Sheffield S3 7HQ, UK; Ziad.Azar@siemensgamesa.com (Z.A.); Richard.Clark@siemensgamesa.com (R.C.); zhanyuan.wu@siemensgamesa.com (Z.Y.W)
* Correspondence: z.q.zhu@sheffield.ac.uk

Abstract: Nowadays, as the application of permanent magnet synchronous machines (PMSMs) and drive systems becomes popular, the reliability issue of PMSMs gains more and more attention. To improve the reliability of PMSMs, fault detection is one of the practical techniques, which enables early interference and mitigation to the faults, and subsequently reduce the impact of the faults. In this paper, the state-of-art fault detection methods of PMSMs are systematically reviewed. Three typical faults, i.e., the inter-turn short-circuit fault, the PM partial demagnetization fault, and the eccentricity fault are included. The existing methods are firstly classified into signal-, model-, and data-based methods, while the focus of this paper is laid on the signal sources and the signatures utilized in these methods. Based on this perspective, this paper intends to provide a new insight into the inherent commonalities and differences among these detection methods, and thus, inspire further innovation. Furthermore, comparison is conducted between methods based on different signatures. Finally, some issues in existing methods are discussed, and the future work is highlighted.

Keywords: demagnetization; eccentricity; fault detection; fault signature; inter-turn short-circuit; permanent magnet; permanent magnet synchronous machine

1. Introduction

Permanent magnet synchronous machines (PMSMs) become growingly popular in industries due to their high efficiency and high torque density [1]. However, reliability has been one of the major concerns that preclude the further promotion of PMSMs in many safety critical applications, such as aerospace, electrical vehicles, and wind power generation. To improve the reliability of PMSMs, a lot of efforts have been put into this subject from the perspective of the topology and design of PMSMs, the condition monitoring, as well as the fault mitigation and fault tolerant control. It has been found that condition monitoring could play a vital role in protecting the PMSM drive system from the catastrophic consequences of the faults [2]. In the area of condition monitoring, fault detection is an important subject, which aims at detecting the faults after their occurrence, thus providing information about the type, location, and scale of faults for subsequent emergency operations. On most occasions of online fault detection, the rapidness of detection is also required to reserve enough reaction time.

Extensive literature has been published about fault detection of PMSMs, covering a wide range of faults. In general, the faults in PMSMs could be classified into 3 categories based on the failure parts, including electrical faults, mechanical faults, and magnet faults [3], as shown in Figure 1. Electrical faults can be further classified according to the faulty components as winding faults, inverter faults, and sensor faults. Mechanical faults include rotor eccentricity, rotor misalignment,

 doi:10.20944/preprints202412.1988.v1

bearing faults, etc. Magnet faults consist of magnet mechanical damage, uniform and partial demagnetization, etc. Winding faults can be further classified according to the failure modes, including inter-turn short-circuit (ITSC) faults, phase-to-phase and phase-to-ground faults, open circuit faults, high resistance connection (HRC) faults, etc.

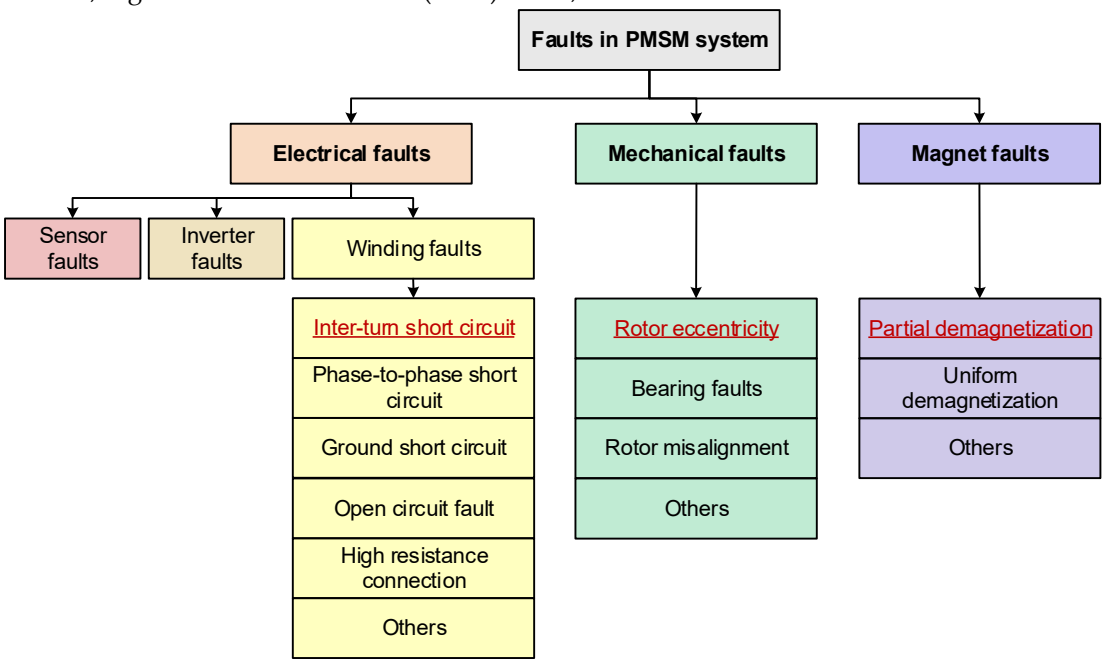

Figure 1. Classification of faults in PMSM drive system.

Several review papers about fault detection have been published. A very comprehensive review is presented in [3] about the fault detection methods. The detection methods are generally classified into 3 categories, signal-based, model-based, and artificial intelligence (AI)-based methods. Diverse kinds of faults are covered in [3] including ITSC fault, magnet faults, and several kinds of mechanical faults. Special attention is paid to the application of advanced signal processing and AI algorithms, nevertheless, lack of analysis about the signal sources. This could be vital because the available signals might vary dramatically among different applications, and thus, the corresponding fault signatures and the analysis methods might be completely different from each other. In [4], the focus is laid on the detection methods, whereas the corresponding fault signatures are not summarized. Several detailed surveys are accomplished about the detection of ITSC [5], demagnetization [6], and eccentricity [7] faults. However, these papers concentrate more on one fault, thus failing to reveal the common features and differences among these faults, which is critical for distinguishment among these faults. In summary, existing review papers are not systematic and detailed enough. Hence, the target of this paper is to provide a more comprehensive review about fault detection of PMSMs in the perspective of the signals and their signatures.

In this paper, the detection methods of three typical faults in PMSMs are reviewed, i.e., the ITSC fault, PM partial demagnetization (PD) fault, and eccentricity fault, because they are very common while difficult to detect. The detection methods of each fault are classified into 3 major categories, i.e., the signal-based, model-based, and data-based methods [3,4,8], as illustrated in Figure 2. Signal-based methods mainly concentrate on extracting the fault-related features of signals directly or indirectly. Model-based methods treat the fault as a variation of the model of motor, hence using various ways to observe the variation of model. Data-based methods utilize the algorithms of machine learning, trying to extract high dimensional hidden information about fault features from the data. Figure 3 concludes the basic principles of signal-, model-, and data-based methods, from the perspective of the general fault detection procedure, i.e., feature extraction and decision-making process.

 doi:10.20944/preprints202412.1988.v1

Furthermore, this paper specifically classifies the papers in literature according to their signal sources and fault signatures, intending to provide a unique insight into the state-of-art techniques for fault detection of PMSMs and their general issues, as shown in Figure 2..

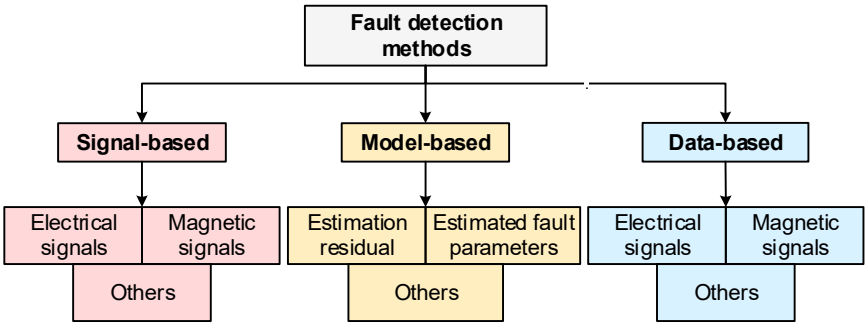

Figure 2. Classification of detection methods for ITSC, PD, and eccentricity faults.

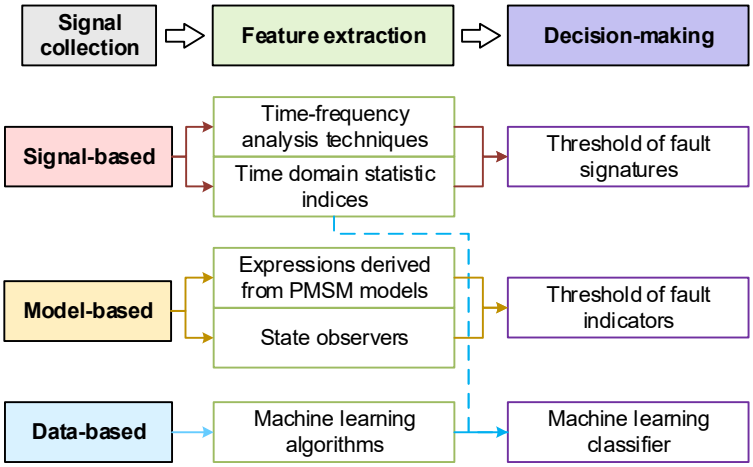

Figure 3. Illustration of fault detection procedure of signal-, model-, and data-based methods.

This paper is organized as follows. Section 2, 3, and 4 discuss the detection methods of ITSC fault, PD fault, and eccentricity fault, respectively. Section 5 discusses some differences in the detection methods of these three faults. Section 6 concludes the paper and presents the future work.

2. Inter-Turn Short-Circuit Fault Detection

2.1. Background

The ITSC fault is the short-circuit between one or a few turns of a winding due to the inter-turn insulation degradation and breakdown. The ITSC fault may be the result of various factors including high winding temperature, mechanical stress, transient overvoltage, etc. When the ITSC fault occurs, the broken insulation part forms a short-circuit path shown in Figure 4 (a). The residual resistance on the short-circuit path can be modelled as a resistance R_f parallel to the short-circuit part of winding. The equivalent circuit of PMSMs with the ITSC fault is shown in Figure 4 (b), where the ITSC fault is assumed in phase A without losing generality.

Preprints.org (www.preprints.org) | NOT PEER-REVIEWED | Posted: 24 December 2024 doi:10.20944/preprints202412.1988.v1

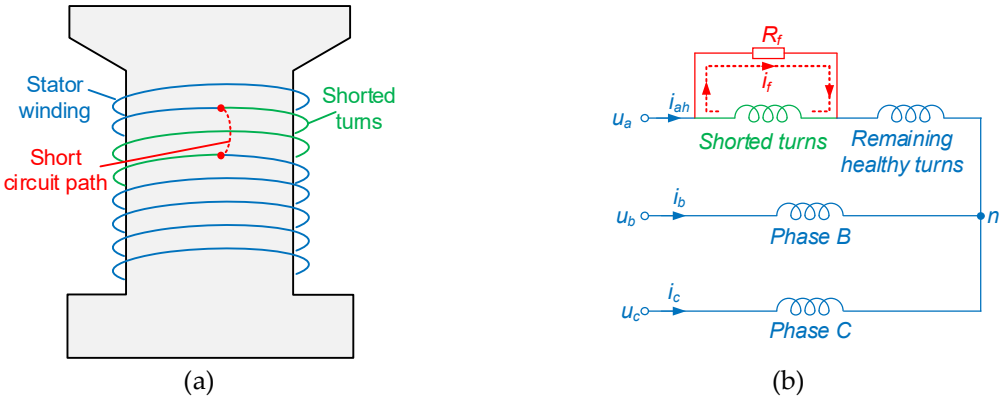

Figure 4. Illustration of ITSC fault. (a) Illustration; (b) Equivalent circuit.

As shown in Figure 4 (b), a large circulating current i_f will flow through the short-circuit resistance R_f as well as the shorted coil L_{af}, causing an extremely high temperature in the local area. High temperature can further accelerate insulation degradation, which may lead to the development of ITSC fault in the manner of avalanche, resulting in more serious fault such as phase-to-phase or phase-to-ground short-circuit [2]. Hence, it is vital to detect the ITSC fault as soon as possible.

However, ITSC fault detection is not easy. The high circulating current does not flow through the regular phase current sensors so that phase currents only contain insignificant fault-related features. Thus, numerous methods are developed to extract and magnify the fault-related features from all types of signals in electrical machines.

2.2. Signal-Based Methods

The signal-based methods refer to those concentrating on extracting explicit signatures from specific signals with time or frequency analysis techniques. The signals adopted for fault detection can be either common electrical signals available in a PMSM drive system, or signals obtained with extra sensors such as Hall sensors or search coils. Generally speaking, the signal-based methods can be grouped as electrical-signal-based and magnetic-signal-based. Obviously, the signatures in electrical signals and magnetic signals are different. Thus, they have different SNR, advantages and disadvantages. The detailed classification is shown in Figure 5.

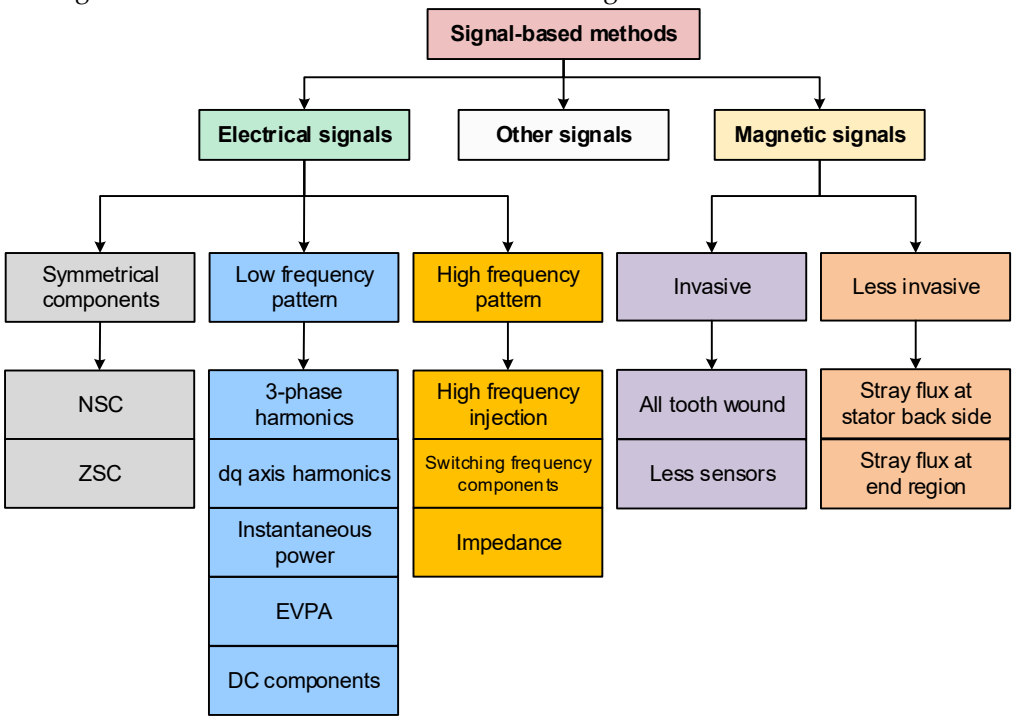

Figure 5. Classification of signal-based methods for ITSC detection.

 doi:10.20944/preprints202412.1988.v1

2.2.1. Electrical Signals

Electrical signals generally include voltage and current signals. Sampled current signals are commonly available in PMSM drive system due to the need of close-loop control. As for voltage signals, usually the reference voltage signals are used, while extra voltage sensors are usually required to sample the zero sequence voltage component (ZSVC). In general, the methods based on electrical signals can be grouped according to the type of signatures:

a) Symmetrical component

Symmetrical component analysis is one of the common ways to detect asymmetry in machines [2,9], where negative sequence component (NSC) and zero sequence component (ZSC) emerge in addition to positive sequence component (PSC). Obviously, ITSC fault introduces asymmetry in stator winding, and thus, ZSC and NSC can be found in either machine voltages or currents. A method based on the ZSC in voltage (for wye-connect machines) and current (for delta-connect machines) is proposed in [10]. The location of ITSC fault can be decided by examining the phase angle information of ZSC, which is also found able to discriminate HRC and ITSC faults [11]. These methods are further integrated with mitigation methods in [12] and [13]. The similar idea is applied in brushless DC (BLDC) machine with a simple fault severity evaluation method [14], reducing the impact of working condition on fault detection. Laadjal *et al*. [15] propose a fault index defined as the ratio between ZSC, NSC and PSC so that the ITSC fault can be distinguished from unbalanced supply voltage. The algorithm is improved by introducing short-time least square Prony's algorithm to track the fundamental frequency component [16,17]. In [18], the ZSC in voltage is found has better signal-to-noise ratio (SNR) and sensitivity to fault than the 2^{nd} harmonics in q-axis current and the speed harmonics.

Similar to ZSC, NSC will emerge in the voltage or current of machines [19]. Jeong *et al.* [20] successfully utilize the NSC in machine voltages to detect the ITSC fault of PMSMs. It is also discovered that NSC in voltage is more sensitive to ITSC fault and more general, compared to ZSC in voltage, because the amplitude of ZSC in voltage is dependent on the leakage inductance of the machine. Meanwhile, NSC in current can also be utilized to detect ITSC fault [21]. A fault indicator is further proposed in [22], by combining the NSC and PSC in current. The phase angle between NSC and PSC in current is used to locate the ITSC fault. Furthermore, NSC in voltage and current can be utilized at the same time. A novel fault indicator is proposed in [23], which is the phase shift between NSC in the machine voltage and current. The indicator can discriminate the unbalanced load of the PM synchronous generator (PMSG) and the ITSC fault, meanwhile the location of ITSC fault is revealed by the phase angle of the NSC in voltage. Similarly, the NSC in voltage can be also combined with ZSC and PSC to detect ITSC fault [15,24].

b) Low frequency (LF) pattern

On the other hand, frequency pattern of signals usually also contains effective signatures for ITSC detection. From the perspective of the way to obtain frequency pattern, diverse frequency analysis techniques are adopted in existing literature, such as Fast Fourier Transform (FFT) [25–28], orthogonal phase-lock-loop (PLL) [29,30], empirical model decomposition (EMD) [31,32], and wavelet transform [33] , etc.

Meanwhile, existing methods also cover a wide range of fault signatures. For example, 3^{rd} harmonics in phase currents are found feasible for detection [31], thus being tracked with quadratic time–frequency techniques, targeting at fault detection at non-stationary situations. Dogan *et al*. [32] extract 3^{rd} harmonics in phase currents using Gabor transform and Ensemble EMD. Lee *et al*. [27] made a conclusion that the negative frequency part of 3^{rd} harmonics is free from supply imbalance and inherent structural asymmetry, leading to its high robustness. The ITSC fault signatures are selected as $(2k\text{-}1)^{th}$ harmonics in [26], which is a more general fault signature. Naderi *et al*. [25] obtain the fault related frequency signatures in the currents of PMSM through comprehensive theoretical analysis, concluding the capability of each frequency component to distinguish among different faults.

The frequency pattern in dq-axis quantities is also widely applied. It is discovered that ITSC fault introduces 2^{nd} harmonics in dq-axis voltage and currents [34], which can be treated as an alternate

 doi:10.20944/preprints202412.1988.v1

perspective of the same fault signatures with NSC [2]. However, the variation in controller bandwidth will cause re-distribution of the 2nd harmonics between voltage and current [35]. Huang *et al*. [30] introduce a fault index called Rayleigh Quotient so that the 2nd harmonics in voltages and currents can be spontaneously synthesized to reduce the influence of current controller bandwidth. The 2nd harmonics extraction method can be improved by applying a short-time Adaline neural network [36], variational mode decomposition (VMD) [37], and wavelet transform [38]. The transient false alarm is mitigated in [39] through estimated compensation signals calculated according to the mechanical close-loop transfer function. There are also methods using the 2nd harmonics in Extended Park's vector approach (EPVA) [40].

Power, which is essentially the multiple of voltage quantities and current quantities, combines both the signatures from voltage and current. The 2nd harmonic is found appearing in instantaneous reactive power (IRP) when ITSC fault occurs in a PMSM working in motoring mode, while appears in instantaneous active power (IAP) in generating mode [28]. The analysis results show the amplitude of the 2nd harmonics in IRP or IAP is sensitive to working conditions. Consequently, the look-up-table (LUT) is adopted to make fault decision. Similar detection method is proposed in [41], where the 2nd harmonics is observed in instantaneous power of a synchronous generator.

Information in the amplitude and phase angle of the fundamental frequency component in phase voltages or currents, i.e., the DC components in dq-axis quantities, are utilized in some papers for ITSC fault detection and discrimination from other faults. The voltage vector variation in dq-axis is used as the fault indicator in [42]. The static eccentricity fault, PM PD fault and ITSC fault cause the voltage vector deviating from healthy vector in different direction. Meanwhile the deviation of current angle is found increasing when ITSC fault occurs while demagnetization causes current angle decreasing [43]. Similarly, the torque angle is utilized in [44], which is essentially the angle between voltage vector and the d-axis. The amplitude and phase differences among $\alpha\beta$ fundamental frequency currents are considered together in [45]. It is worth mentioned that recently, the fundamental frequency components in xy subspace of dual-three-phase PMSM (DTPPMSM) is found feasible to detect and locate the ITSC fault [29,46–48].

c) High frequency (HF) pattern

Previously mentioned papers mainly concentrate on frequency pattern in LF range. As for pattern in HF range, two types of methods are developed, i.e., methods based on the switching frequency components and those based on the HF injection.

Switching frequency components exists in switching-inverter based drive system. It is a naturally embedded excitation source providing useful information for fault detection. Sen *et al*. [49] observe that the admittance of phase winding increases at the HF region after ITSC fault happens. Hence, switching frequency ripple is adopted as the HF test signal to obtain the HF impedance of winding. Similar idea is also investigated in [50]. Hu *et al*. [51] model and analyse the pulse-width modulation (PWM) signals in a PMSM and obtain the analytical expression of PWM ripple current. The analytical expression as well as simulation shows that the amplitude of PWM ripple current of the faulty phase increases when ITSC fault occurs. A fault index is further proposed defined as the ratio of the $2f_{switching}$ component in adjacent phases. Same principle is adopted in [52], while its capability to distinguish between high resistance connection (HRC) and ITSC fault is discovered. HRC fault only causes resistance asymmetry, hence insensitive to HF voltage, while ITSC causes inductance variation, hereby discrimination of two kinds of fault. The method is improved by combined the ZSVC and switching frequency component analysis [53]. The fundamental component of ZSVC is used to detect asymmetry in stator, while the HF component in ZSVC is used to distinguish between HRC and ITSC fault. Meanwhile, GAO *et al*. [54] combined the NSVC and switching frequency component analysis. Wang *et al*. [55] compare interior PMSMs (IPMSMs) and surface-mounted PMSMs (SPMSMs), where the saliency ratio is proved to be insignificant to the switching frequency and its sideband in current spectrum.

Switching frequency components in voltage rely on the modulation index, thus being influenced by working conditions. On the other hand, by injecting HF voltage or current, the excitation source becomes independent from working conditions, making fault signatures much more consistent

 doi:10.20944/preprints202412.1988.v1

across different working conditions. A method based on HF rotating current is proposed to distinguish between HRC and ITSC fault [56]. The injected frequency component is extracted from ZSVC. Xu *et al*. [57] inject specially designed HF current so that injected current only flow through two phases at one time. The line voltage difference when injecting different pairs of phases is selected as the fault indicator. Other than current injection, rotating square wave voltage is injected in [58,59] and the differences of the HF response in three phases are selected as the fault features. Different kinds of signal injection methods, including rotational voltage, static pulsating voltage, rotational pulsating voltage, and rotational current are systematically compared in [60]. The rotational voltage injection with constant amplitude is found with more significant fault features while simpler injection structure than the others. HF injection method is improved in [61] by replacing the zero voltage vector in the output of space vector PWM (SVPWM), which results in a spatial asymmetrical distributed rotating HF voltage. The capability of locating ITSC and HRC faults with high frequency injection is further extended in [62].

Impedance can be calculated based on signal injection. It can be seen as another perspective to evaluate the ITSC fault. Qi *et al*. [63] find that ITSC fault and eccentricity have different influence on the impedance over the whole region of magnetic working points, which can be used to distinguish these two faults. Another different way of utilizing impedance information is presented in [64], where the resistance of phase winding is used as the fault indicator. When ITSC fault occurs, the resistance of corresponding phase reduces, leading to reduction of *d*-axis resistance, which is estimated by injecting DC voltage at standstill condition.

d) Others

Apart from the aforementioned methods, there are various ways of extracting fault signatures from current and voltage. Hang *et al*. [65] provide a novel method that uses the differences among three phase current amplitude as the fault indicator. Obeid *et al*. [66] manage to detect the distortion in phase current or voltage waveforms caused by intermittent ITSC fault using adaptive wavelet transform. Cost function of the model predictive control system is utilized as a fault signal source in [67]. Discrete wavelet transform (DWT) is adopted to analyse the cost function signal, since it is non-stationary signal. ITSC fault is detected by monitoring the normalized energy-related feature vector calculated from the wavelet transform coefficients. Skewness of currents [68], current envelope [69], model signal of phase currents [70], are also found effective for detection of ITSC fault.

2.2.2. Magnetic Signals

Unlike electrical-signal-based methods, magnetic-signal-based fault detection methods extract fault signatures through the magnetic field. These methods provide a different view of the ITSC fault. As shown in Figure 6, different mounting places of sensors require different level of modification to the machine. According to the significancy of modification, magnetic-signal-based methods can be classified into two kinds, i.e., invasive methods and less-invasive methods. Since the flux distribution varies in space, the signals captured in different places are certainly different, and thus, different fault features are discovered with these two kinds of methods.

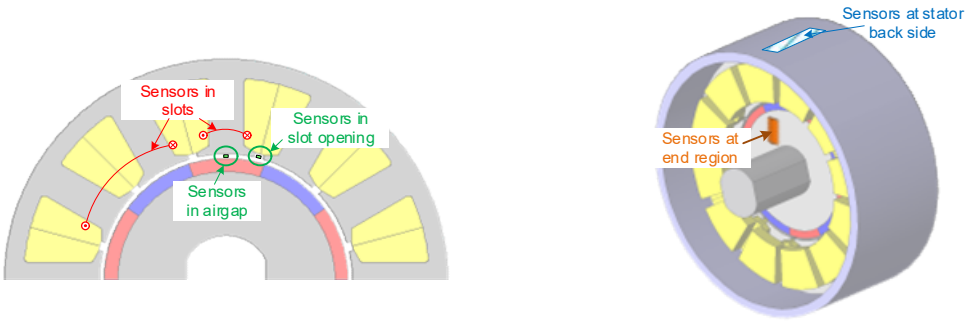

(a) (b)

Figure 6. Illustration of typical mounting placing of flux sensors for fault detection. (a) Invasive methods; (b) Less-invasive methods.

 doi:10.20944/preprints202412.1988.v1

a) Invasive methods

Invasive methods place the sensors on the main flux path of the machine, as shown in Figure 6 (a). Thus, sensors are usually placed in the slots [71] [72], stator yoke [73], around the tooth coils [74], etc., meaning that significant modification of the machine is required. Da *et al*. [71] utilized the search coils on all tooth for the detection of various faults. The polar diagram is then drawn to see the distortion of airgap flux linkage due to ITSC fault. Similarly, Zeng *et al*. [75] also use search coils wound on tooth. The frequency components $(2h_k\pm1)f_e$ (h_k is the carrier wave ratio) are found having high SNR, and a fault index based on these two components is proposed.

On the other hand, only 6 search coils are required in [72] by setting the coil pitch of search coils the same as the coil pitch of phase windings. The NSC with frequency of $2f_s\pm f_e$ component is extracted as the fault indicator, where is f_s the switching frequency. Furthermore, a universal design method for search coil structure is developed in [76] considering the reliability, sensitivity, SNR, and positioning capability of the induced voltage.

b) Less-invasive methods

Compared with the invasive methods, less-invasive methods make less significant modifications to the machine. The sensors are usually placed at the end region or outer side of the stator back iron, as shown in Figure 6 (b). Liu *et al*. [77] build and analyse the magnetic equivalent circuit model of a PMSM and found that the stray flux at stator back side changing with the magnetomotive force (MMF) of windings. Thus, tunnelling magneto-resistive (TMR) sensors are placed at the stator back side to obtain the stray flux density. Polar diagram is drawn to discover the distortion in spatial distribution. A similar method using only two search coils at symmetrical position of stator back side is proposed in [78]. Pearson correlation coefficient is adopted to analyse the induced voltage in two search coils. Gurusamy *et al*. [79] specifically use the 3rd harmonics in stray flux to detect ITSC fault in PMSMs because the fundamental frequency component may lead to false negative error. Eldeeb *et al*. [80] propose a different method by utilizing the switching frequency components in the stray flux, where an antenna placed at relatively far away from the machine is used to extract the switching frequency and its odd number multiple components.

The housing of the machine may affect the stray flux distribution at the stator back side. In such case, placing sensors at the end region is an alternative way. Assaf *et al*. [81] analyse the spectrum of the axial stray flux as well as the sensitivity of different frequency components to ITSC fault and unbalanced supply. Lamim *et al*. [82] place two stray flux sensors at the end region, which are orthogonal to each other. Orbit diagram is used to illustrate the distortion of leakage flux linkage. Kumar *et al*. [83] combine temperature and the leakage flux density together for ITSC fault.

2.2.3. Other Signals

Other signals are also utilized for ITSC fault detection, such as mechanical signals [84], and temperature signals [83,85]. For example, since the ITSC fault leads to harmonics in currents, it can be expected that these will excite corresponding mechanical response. Hence, the 4th harmonics in speed signals [37,86,87] and vibration signals [84] are investigated for ITSC fault detection.

2.2.4. Comparison

Table 1 concludes the general advantages and disadvantages of different kinds of signal-methods discussed in this section.

Table 1. Comparison among signal-based methods of ITSC detection.

Signal Types	Fault Indicator Types		Advantages	Disadvantages
Electrical signals	Symmetrical components	ZSC	+ Suitable for online detection + Irrelevant to winding topology & pole-slot combination	- Troublesome to measure ZSC voltage

Preprints.org (www.preprints.org) | NOT PEER-REVIEWED | Posted: 24 December 2024 doi:10.20944/preprints202412.1988.v1

Magnetic signals	LF pattern	NSC	+ Irrelevant to winding topology & pole-slot combination + Higher amplitude than ZSC + Easier to obtain	- Affected by unbalanced input
		3-phases harmonics	+ Easy to obtain + Readily integrated in control system	- Difficult for transient process - Usually high computational burden - Influenced by winding topology
		dq-axis harmonics		
		Impedance	+ Less influenced by controller bandwidth	- Influenced by saturation/temperature
		Instantaneous power	+ Less influenced by controller bandwidth	- Sensitive to load & speed - Low sensitivity at no-load condition
		Others	+ Easy to obtain	- Not suitable for transient process
	HF pattern	Injection	+ Steady sensitivity + Suitable for wide range of load & speed	- Vibration & noise - Influence on control performance
		PWM related	+ High SNR	- Low sensitivity at no-load condition - Difficult to sample PWM ripple current
	Invasive		+ High SNR	- Invasive - Usually need many sensors
	Less-invasive	Stator back side	+ Less invasive	- Influenced by housing
		End region		- Low SNR

2.3. Model-Based Methods

Instead of explicitly extracting certain time or frequency domain features from signals, model-based methods utilize the mathematical or finite element method (FEM) models of PMSMs to estimate fault-related quantities. Compared with signal-based methods, model-based methods rely more on the machine parameters, but are usually more suitable for transient conditions.

To better reveal the essential differences between these methods, in this paper model-based methods are classified according to their observed signatures. For ITSC fault detection, the commonly used signatures include estimation residual, estimated shorted turn ratio, etc., as shown in Figure 7.

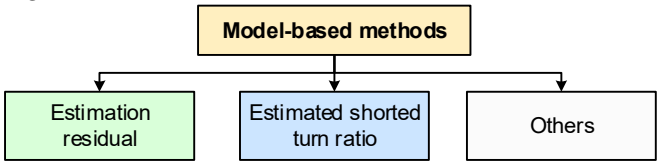

Figure 7. Classification of model-based methods for ITSC detection.

2.3.1. Estimation Residual

Healthy PMSM models are commonly used in this category of detection methods. When the ITSC fault occurs, the model of real machine becomes different from the assumed healthy model, causing errors in the estimation results. Hence, the estimation errors can be used as a fault indicator.

 doi:10.20944/preprints202412.1988.v1

Three phase current residuals are estimated with open-loop calculation in [88]. Meanwhile, a $\alpha\beta$ current observer with feedback is adopted in [89] to calculate current residuals considering the non-linearity of inverter model and unbalanced inductance. Mazzoletti *et al*. [90] further consider the influence of parameter errors. It is proved that NSC in current estimation residual is independent to parameter errors, hence being used as fault indicator to reduce the influence of the parameter variation. The NSC of the residual is also selected as the fault indicator in [91], but the current estimation is achieved with the assistance of FEM so that saturation effect can be considered. The FEM model provides the relationship between *dq*-axis flux linkages and currents. Similar principle is adopted in [92] while the influence of working conditions is mitigated with a LUT. Mahmoudi *et al*. [93] use the Luenberger observer to estimate the *dq*-axis currents. The NSC in the estimation residual is still used as the fault indicator. A full-order Luenberger observer [94] and the extended Kalman Filter [95] have also been investigated for residual calculation. To better account for parameter uncertainty and nonlinearity, digital twin models are used to obtain the current residuals [96].

Similar to current residuals, voltage residuals are also utilized. Hang *et al*. [97] model the PMSM under the ITSC fault condition with two terms of voltage disturbances at *dq*-axis, , and use the Luenberger observer to estimate the voltage disturbances. The sum of two voltage disturbances is taken as the fault characteristics signal, and the 2nd harmonics in it is used as the fault indicator. Similarly, Du *et al*. [98] estimate the disturbance in back-EMF with an extended state observer and extract the 2nd PSC in the disturbance as the fault indicator. A five-phase PMSM is investigated in [99], where the voltage disturbances in all phases are estimated.

Other than currents and voltages, various physical quantities can also be estimated to monitor the deviation of machine model due to occurrence of fault. Sarikhani *et al*. [SAR13] estimate the back-EMF of PMSM, and similarly, take the residual of estimation as the fault indicator. However, the fault index is set to the linear average of residual normalized against speed. Cui *et al*. [100] estimate the electromagnetic torque using torque equation at healthy condition. The estimation error is obtained by subtracting estimation value with the real value measured with torque transducer. Through theoretical analysis, the DC component in residual is found only exist when the ITSC fault occurs, thus being used as the fault indicator. Xu *et al*. [101] analyse the model of sensorless SPMSM with ITSC fault considering the inverter nonlinearity and the current measurement error. The residual voltages in estimated *dq*-axis contain various harmonics when ITSC fault happens. With proper harmonics elimination algorithm, the 8th harmonics in voltage estimation residual is selected for ITSC fault detection.

Upadhyay *et al*. [102] estimate the flux linkage in *dq*-axis and draw the XY diagram to observe the trace of flux linkage. By extracting the DC component in the flux linkage trace variation, the fault can be detected and located.

For DTPPMSM, Yang *et al*. [103] utilize the difference of voltage vectors of two sets windings to detect the ITSC fault.

Furthermore, the model-based method can be combined with high frequency injection method for better SNR, by estimating the high frequency injection residual [104,105].

2.3.2. Estimated Shorted Turn Ratio

This kind of methods utilize the PMSM model with ITSC fault. The faulty model contains the shorted turn ratio as a parameter. Thus, the short-circuit ratio can be estimated with the information in machine voltages or currents, either through open-loop expressions [106], or close-loop observers [107,108].

Aubert *et al*. [107] build a PMSM model consisting of the standard PMSM voltage equations and the short-circuit loop voltage equation. Kalman filter is adopted to estimate the shorted-turn ratio of each phase. Sayed *et al*. [108] take similar way, but also compare the performance of extended Kalman filter and the unscented Kalman filter. Furthermore, Hidden Markov model is adopted in [109] to estimate the range of shorted turn ratio and short-circuit resistance.

 doi:10.20944/preprints202412.1988.v1

2.3.3. Others

Except for the estimation residual and the estimated shorted turn ratio, several other fault indicators have also been investigated, such as estimated torque [110], the probability distribution function of estimated machine parameters [111], speed estimation residual [112], etc.

2.3.4. Comparison

Table 2 concludes the general advantages and disadvantages of different kinds of model-based methods discussed in this section.

Table 2. Comparison among model-based methods of ITSC detection.

Signatures	Advantages		Disadvantages	
Estimation residual	+ Less computational burden	+ Suitable for non-stationary condition	- More estimated variables	- Dependent on machine parameters
Estimated shorted turn ratio	+ Easy to evaluate fault severity			
Others				

2.4. Data-Based Methods

Compared with signal- and model- based methods, data-based methods generally use a significantly larger amount of machine operating data. Fault signatures in the data are extracted and analyzed implicitly through machine learning process, while the machine model and explicit fault signatures are usually less important.

Data-based methods can be classified according to the signals they used: electrical signals, magnetic signals, and other signals, as shown in Figure 8.

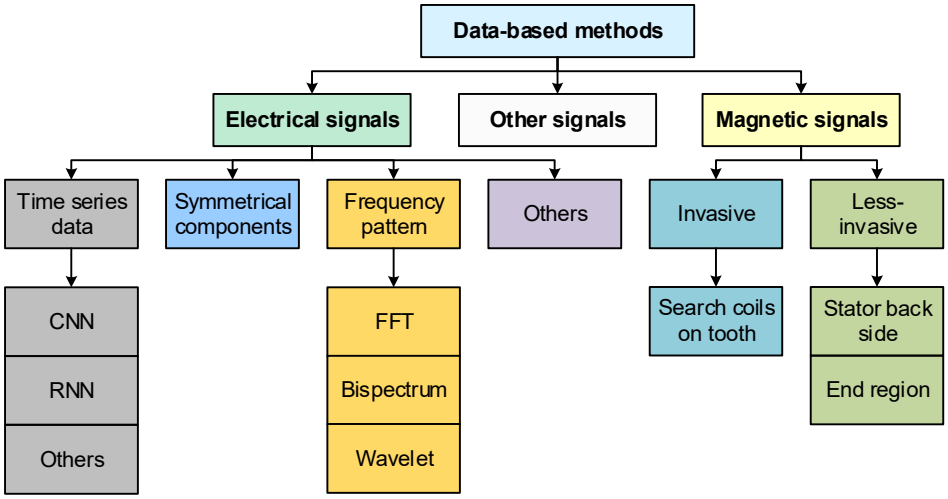

Figure 8. Classification of data-based methods for ITSC detection.

2.4.1. Electrical Signals

Machine learning algorithms put no limit on the input data forms. Some algorithms such as CNN or recurrent neural network (RNN) can directly process the time-series data, and the implicit fault features are automatically learnt from the training data. In contrast, fault signatures in the time series data can also be processed with signal analysis tools such as FFT, and the fault-related information in the results can be subsequently extracted with machine learning algorithms. Thus, the methods are further classified according to the forms of input data of machine learning algorithms.

 doi:10.20944/preprints202412.1988.v1

a) Time series data

Data in the form of time sequence can be directly fed into the machine learning algorithms. Thus, the fault signatures are automatically determined and extracted with machine learning process, and then being analysed and classified. In [113], three phase voltage and current signals are directly input into the proposed framework. Multiple feature extraction methods, as well as multiple classification are used in parallel and synergised with the Fisher's ratio. Wang *et al*. [114] manage to detect ITSC fault with two of three phase currents and the deep autoencoder. Furthermore, only one phase current is required in [115].

A wide range of existing methods apply the convolutional neural network (CNN) for fault detection. The convolution layer usually plays a role as the feature extraction methods in the machine learning structure. Compared with traditional spectrum analysis tools such as FFT, the corresponding features are identified and extracted with convolution layer self-adaptively according to the training data, because the convolution core is obtained through training process. In [116], a method based on CNN is proposed, where time series of three-phase currents compose a $3\times n$ array as the input of CNN. Shih *et al*. [117] compare the performance of SVM and CNN on ITSC fault detection. Time series of q-axis voltage and current are used as the input of SVM, while the waveforms of them are converted into 2D image and fed into CNN. A conclusion is made that SVM which is assisted with mathematical model of PMSM requires much less data. On-Bayesian-optimization-based residual CNN is applied in [118] to reduce network depth and avoid degradation effect when feeding time series data into CNN. A residual dilated CNN is applied in [119] combined with transfer learning techniques. Some other applied methods such as deep Q-network [120] and stacked autoencoder [121], also have one or multiple convolutional layers.

Apart from CNN, transformer neural network [122], RNN [123], etc., can also learn the features from time-series data.

b) Symmetrical components

Instead of directly feeding three phase current signals, NSC and PSC are used as input for a neural network in [124]. Similarly, an attention-based RNN is adopted in [123] to analyze the NSC, PSC and speed. Meanwhile, Pietrzak *et al*. [125] take NSC and PSC as the input of the K-Nearest Neighbour (KNN) algorithm.

In [126], an efficient method based on stacked sparse autoencoders and Siamese networks is proposed to reduce the amount of data required for training. Seven kinds of signals and features are integrated into the dataset, including three-phase current, NSC and PSC in current, NSC impedance, and electronic torque.

c) Frequency pattern

Machine learning algorithm can also process the spectrum of three phase currents [127,128] or dq currents [129]. Specifically, Pietrzak *et al*. [130] use Bisepctrum analysis to pre-process three-phase currents. The result of Bispectrum analysis is a 2D image, which is then fed into a CNN for further feature extraction. Meanwhile, other time-frequency analysis techniques such as the wavelet transform [131] are also adopted.

d) Other features

The image of Park's vector trajectory is used as the input of neural network in [132]. In [133], 15 features are extracted from current signals to build up the dataset, including mean value, maximum value, root-mean-square (RMS) value, etc. In [134], the difference between two of three phase currents are obtained to enhance the fault signatures.

The estimation residual of q-axis current based on Luenberger observer is used in [135] so that the information of PMSM model can be incorporated into machine learning process.

2.4.2. Magnetic Signals

Search coils are placed on tooth to capture the abnormality in airgap flux density distribution due to the ITSC , eccentricity and partial demagnetization fault in [136], where the induced voltage is processed into image by short-time Fourier transform. Meanwhile, the stray flux density in end region [137] and at the stator back side [138] are also investigated.

 doi:10.20944/preprints202412.1988.v1

2.4.3. Other Signals

Apart from the electrical and magnetic signals, many other signals are also used for ITSC detection. For example, torque signal is combined with currents in [120]. Speed signal is combined *dq* voltage and currents in [129] to reduce the influence of controller bandwidth. Furthermore, the input current on the power side [139] and the vibration signals [140] are also investigated.

2.4.4. Comparison

Table 3 concludes the general advantages and disadvantages of different kinds of model-based methods discussed in this section.

Table 3. Comparison among data-based methods of ITSC detection.

Input Data Types		Advantages	Disadvantages
Electrical signals	Time series	+ Non-invasive + No need for choosing signal analysis tools	- Difficult to integrate the information about widely adopted fault harmonics
	Symmetric components	+ Non-invasive + High sensitivity	- May be limited by the information in the extracted features
	Spectrum		
Magnetic signals	Airgap flux density	+ High sensitivity	- Invasive
	Stray flux density		- Relatively low SNR

3. Partial Demagnetization Detection

3.1. Background

Demagnetization of a magnet means the magnetic property of this magnet degrades. Once the applied field strength exceeds the knee-point of the B-H curve of a PM, as shown in Figure 9, the working point of the PM will not recover following the original B-H curve but will follow the recoil line. This means that the remanence is reduced from B_{r1} to B_{r2}, in other words, the PM is demagnetized. Generally, high temperature and large armature field are the main cause of demagnetization fault [141]. The demagnetization severity of a PM is usually reflected in its remanence B_r, which decreases as the severity of demagnetization increases.

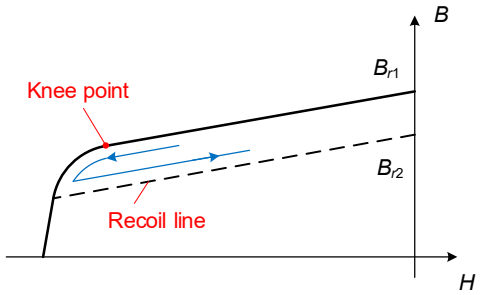

Figure 9. Illustration of demagnetization curve of a PM [142].

In the area of fault detection, PM demagnetization faults are usually classified into two categories: uniform demagnetization (UD) and PD. UD means all PMs in a PMSM are demagnetized uniformly, while PD means only one or a few PMs are demagnetized, and the severity of demagnetization can be non-uniform. In recent research, PD detection gains more attention due to its commonness and difficulties in detection. Hence, this paper concentrates most on PD detection rather than UD detection.

 doi:10.20944/preprints202412.1988.v1

PD causes unwanted harmonics in the back-EMF and currents, as well as torque ripple, unbalanced magnetic pull, and vibration [3], leading to deterioration in performance and efficiency of the PMSM drive system.

Detection of PD has been widely investigated in the past few decades. The proposed methods can be classified into signal-based, model-based, and data-based, similar to the ITSC detection methods.

3.2. Signal-Based Methods

Classification of signal-based methods for PD detection is shown in Figure 10.

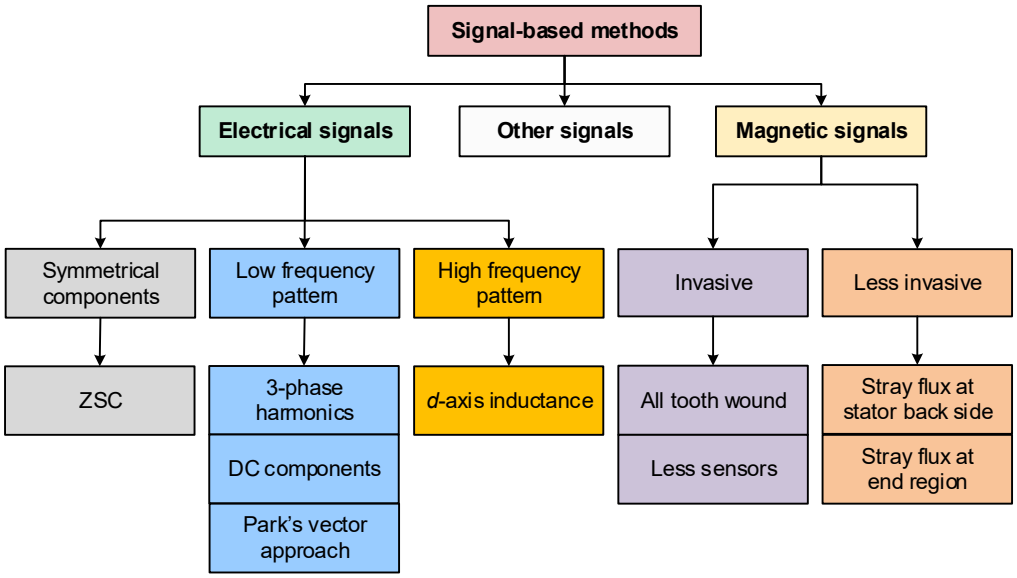

Figure 10. Classification of signal-based methods for PD detection.

3.2.1. Electrical Signals

a) Symmetrical components

Similar to ITSC fault detection, symmetrical component analysis can also be applied in PD detection. The mostly used symmetrical component in PD detection is ZSC. Urresty *et al*. [143] discuss the influence of winding configurations on the spectra of currents and ZSVC of a PMSM with demagnetization fault. It is proved that harmonics appear in both current spectrum and ZSVC spectrum in fractional-slot PMSM in the case of PD. But in integral-slot PMSM, new harmonics may not emerge in current or ZSVC spectrum, depending on the specific winding configuration. It is also discovered in [144] that fractional harmonics in current spectrum related to PD might be cancelled in phase current with certain winding configurations. However, the ZSVC will not be eliminated in such winding configuration, hence eligible for PD detection. Furthermore, Zhan *et al*. [145] extend the ZSC-based methods to DTPPMSM. The drop of the 3rd harmonics in the difference of ZSVC in two set of windings is chosen as the fault indicator for an integer-slot machine, while for other types of machines, the fractional harmonics are used.

b) LF pattern

Fractional harmonics are very frequently used in demagnetization fault detection. When PD occurs, the frequencies of harmonics emerge in three phase currents can be expressed as (1) [146]:

$$f_{PD} = f_e\left(1 \pm \frac{k}{p}\right), k = 1,2,3,\cdots, \tag{1}$$

where f_e is the electrical frequency, p is the pole-pair number, and k is any positive integer.

According to the pole number of a certain machine, the corresponding fault harmonics can be obtained FFT [147]. However, at transient condition, the fundamental frequency components interact with fault-related harmonics [148], causing false alarm. Thus, advanced signal processing techniques

 doi:10.20944/preprints202412.1988.v1

are adopted to track and analysed the harmonics such as wavelet transform [149], box-counting algorithm [150], Vold-Kalman filter [151], T-*f* decomposition [148,152], HHT [153], etc. Other than harmonics in the phase currents, harmonics in *dq* currents are also evaluated for PD detection in [154].

The capability of a certain harmonics to distinguish PD from eccentricity is paid special attention. In [147], the 2/3rd and 4/3rd harmonics emerge in stator spectrum of a 6-poles SPMSM at both PD and dynamic eccentricity fault condition, thus unable to distinguish them. On the other hand, the 1/4th and 1/2nd harmonics are found able to distinguish PD from static eccentricity [155] in a 9-slot 8-pole SPMSM. Amplitude and phase angle of the (1-1/*p*)f_e harmonics are used together to distinguish PD and eccentricity fault. Furthermore, Naderi *et al*. [25] systematically analyse the homopolar frequency components in stator current and conclude the components with the capability to distinguish between PD, eccentricity, and ITSC fault.

The PD-related frequency components are studied comprehensively in [156,146] considering pole-slot combination, double-layer and single-layer winding, as well as skew angle. It is found that the harmonics at triple multiple of mechanical frequency may disappear due to winding configuration. Specifically, in the case when the following criteria is satisfied

$$n_{layer} \times \frac{n_{slot}}{2p} = 3k, k = 1,2,3,\cdots,$$

PD does not create harmonics in stator currents, where n_{layer}, n_{slot}, and p is the number of winding layers, slots, and pole-pairs, respectively. A systematic analysis is presented in [157] about the harmonics in back-EMF at PD and eccentricity conditions.

Apart from harmonics, the variation of current angle [43] and torque angle [44] are found feasible to distinguish PD and ITSC faults, and furthermore, the torque angle can be combined with the voltage vector amplitude to further discriminate PD, SE, and ITSC faults [42].

Methods based on current spectrum, Park's vector approach (PVA), extended Park's vector approach (EPVA) are compared in [158] and the EPVA is found superior in terms of high sensitivity and robustness.

Furthermore, the signatures in the 5th harmonics subspace voltage vector of the DTPPMSM are investigated [159].

c) HF pattern

Generally, very few papers utilize the HF pattern in voltages or currents for PD detection. However, it is found in [160] that the demagnetization can change the saturation level of the machine, and thus, it can be detected by inspecting the *d*-axis incremental inductance. It is also claimed that this method can detect PD fault in the case where machine current signature analysis (MCSA) cannot.

d) Others

Instead of using spectrum analysis, Hong *et al*. [161] use the waveform of currents to detect PD at standstill condition, essentially utilizing the impact of PD on the saturation level of iron core. It is also worth mentioned that Fernandez *et al*. [162] and Reigosa *et al*. [163] managed to utilize the magnetoresistance effect of PM to estimate the magnetization state of PM.

3.2.2. Magnetic Signals

a) Invasive methods

As discussed previously [146], some PD signatures in currents or voltages may not emerge depending on the topology of PMSM. Magnetic-signal based methods can get around that limitation through extracting the fault signatures directly from the flux or flux density.

The radial airgap flux density is analysed at different working conditions in [164], and Hall sensors are placed in the airgap to obtain the corresponding signatures. Search coils wound on each tooth are adopted in [71], and the first-order harmonics amplitudes in each search coil are used. This method is improved in [165] by introducing a more robust fault index, which subtracts the average value of induced voltage in the range of 120° mechanical angle from the original induced voltage waveforms. Multiple harmonics are used to evaluate the severity of PD in [166]. The abovementioned methods require search coils with only one tooth pitch wound on each tooth, which might be too complicated for PMSM with many slots.

 doi:10.20944/preprints202412.1988.v1

A method [167] is proposed by using two search coils placed on the tooth and facing the airgap. Four search coils are placed at the slot opening in [168]. In [169], six search coils with one pole pitch are placed in stator slots of a 36-slot 4-pole machine. The induced voltage in the search coils is found containing $(2k+1\pm2/p)^{th}$ order harmonics when PD occurs. Rafaq *et al*. [170] find out that for PD detection, only one search coil on the tooth is essentially enough, because the demagnetized PM can be continually scanned by the search coils when the rotor is rotating. Skarmoutsos *et al*. [171] place a search coil in slots with coil-pitch being exactly four pole pitch. Consequently, the induced voltage will be zero at healthy condition, resulting in a better signal-to-noise ratio (SNR). When PD occurs, the peak-to-peak value of induced voltage is used to calculate the fault index.

Besides in [172], the search coils are wound at the stator yoke. Two search coils are placed at the bottom of two slots, whose distance is exactly one pole-pitch and connect with each other in a way to makes sure the ideal output is zero at healthy condition. Chen *et al*. [173] improved this method by adding another search coil which is also one pole-pitch away. Totally 8 search coils on the stator yoke are used in [73] to achieve discrimination between the PD and ITSC faults. Furthermore, the search coil on the rotor is also investigated in [174].

In [175], a special type of demagnetization was discussed, where the trailing edge of PM is demagnetized. It is demonstrated that monitoring airgap flux has the detectability of this type of demagnetization.

b) Less invasive methods

The stray flux at the stator back side contains similar harmonics and signatures as airgap flux [79,176]. Goktas *et al*. [177] apply two flux-gate sensors located behind the tooth and behind the slots respectively. A circumferentially equidistant array of eight TMR sensors are placed outside the stator in [178]. Time domain fault index based on the envelope and the average of stray flux density is calculated, which shows better performance than methods based on machine current signatures.

The stray flux in the end region can also be utilized. Hall sensors placed at the end region close to the PM are used to detect demagnetization [179]. The method is improved in [180] using the ZSC flux in the end region, which presents higher sensitivity. Park *et al*. [181,182] reduces the amount of Hall sensors to one, and further discuss the feasibility of fault detection with digital Hall sensors. The basic principle is that if the rotor PMs are not symmetrical due to local demagnetization or damage, the flux measurement of the Hall sensor will be smaller when the demagnetized PM passes the Hall sensor.

3.2.3. Other Signals

PD causes harmonics in the spectrum of currents and voltages, consequently causing harmonics in torque, i.e. torque ripple. In [183], the amplitude of $(\lambda\pm\xi/p)^{th}$ harmonic in torque is chosen as the fault index, where λ and ξ are integers, p is the pole-pair number. Furthermore, the 0.25^{th} harmonic in vibration signal is used in [184].

3.2.4. Comparison

Table 4 concludes the general advantages and disadvantages of different kinds of signal-based methods discussed in this section.

Table 4. Comparison among signal-based methods of PD detection.

Signal Types	Fault Signature Types		Advantages	Disadvantages
Electrical signals	Symmetrical components	ZSC	+ Irrelevant to winding topology or machine topology	- Difficult to measure
	Frequency pattern	Spectrum	+ Non-invasive	- Highly dependent on winding topology & machine topology

Preprints.org (www.preprints.org) | NOT PEER-REVIEWED | Posted: 24 December 2024 doi:10.20944/preprints202412.1988.v1

		Impedance	+ High SNR	- Highly influenced by temperature
	Others	Waveform pattern	+ Intuitive & simple	- Highly influenced by saturation
Magnetic signals	Invasive	All tooth mounted	+ Distinguishable among different faults + Intuitive	- Large amount of sensors
		Few teeth mounted	+ Fewer sensors	- Relatively difficult to distinguish PD from other faults
		Pole-specific search coils		
	Less-invasive	Stator back side	+ Less invasive	- Affected by housing
		End region		- Difficult to accurately mount the sensors

3.3. Model-Based Methods

Classification of model-based methods for PD detection is shown in Figure 11.

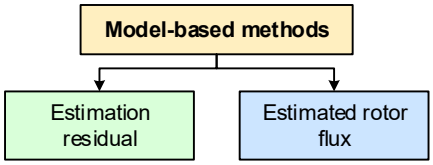

Figure 11. Classification of model-based methods for PD detection.

3.3.1. Estimation Residual

In [185], the airgap flux density is estimated in real-time through the analytical equations assisted with offline FEM model and compared with the measured signal obtained with Hall sensors. The deviation is then processed with wavelet transform to extract the target frequency, followed by a classifier. Bisschop *et al*. [186,187] managed to build up the analytical expression of the induced voltage in search coils. Then, the predicted induced voltage is compared with measured value, and the deviation is used to evaluate the severity of PD.

3.3.2. Estimated Rotor Flux

Roux *et al*. [188] estimate *d*-axis flux linkage with the voltage equation of PMSM and monitored the decreases in the estimated value. Moon *et al*. [189] present a method to estimate the PM flux and the L_d, L_q at the same time. The variation in PM flux is combined with deviation of L_d and L_q to detect PD. Zhu *et al*. [190] estimate the rotor flux by using torque ripple as the input of rotor flux estimation algorithm. Liu *et al*. [191] also estimate the rotor flux, while simultaneously monitoring the HF *d*-axis inductance to discriminate the eccentricity and the PD faults. Han *et al*. [192] further take the variation of parameter into consideration, and successfully separated the estimated quantity irrelevant to parameter error. Rotor flux linkage can also be estimated with PWM voltage measurement [193] to exclude the influence of inverter nonlinearity.

For DTPPMSM, PD detection can be achieved by monitoring the flux linkage in the 5^{th} harmonics subspace [194].

3.3.3. Comparison

Table 5 concludes the general advantages and disadvantages of different kinds of model-based methods discussed in this section.

 doi:10.20944/preprints202412.1988.v1

Table 5. Comparison among model-based methods of PD detection.

Signal Sources	Signatures	Advantages		Disadvantages
Voltage/Current	Estimated rotor flux	+ Non-intrusive	+ Suitable for transient condition	- Unable to locate fault - Low sensitivity - Essentially influenced by machine topology
Flux signal + Voltage/current	Estimation residual	+ High sensitivity		- High cost of flux sensors - Invasive

3.4. Data-Based Methods

Classification of data-based methods for PD detection is shown in Figure 12.

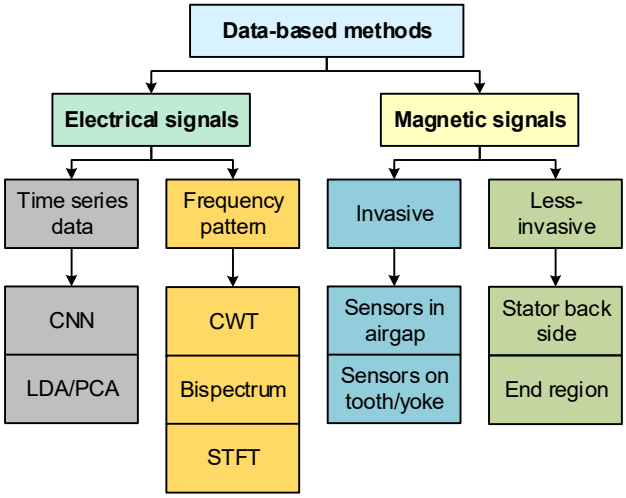

Figure 12. Classification of data-based methods for PD detection.

3.4.1. Electrical Signals

Skowron *et al*. [195] target at detect the ITSC fault and the PD fault at the same time. The raw current signals are constructed as a 20×25×3 array and fed into a CNN. Similar principle is adopted in [196], while transfer learning technique is integrated into the diagnosis framework. Chen *et al*. [135] also adopted CNN to distinguish ITSC and PD, but processed the current and voltage signals with model-based method, and fed the CNN with q-axis current residual. Other than CNN, linear discriminant analysis and principle component analysis are combined with variational autoencoder in [73] to extract implicit features in current signals.

The method proposed in [197] convert both voltage and current signals into images, and then process them with local binary pattern texture analysis. The extracted features are then classified by KNN algorithm. Bispectrum is adopted to convert the three phase currents into images in [198] to detect eccentricity and PD faults. Continuous wavelet transform (CWT) is combined with ResNet in [115], and the short-time Fourier transform (STFT) is combined with KNN and multilayer perceptron in [199].

It is worth noting that because of the strong capability of machine learning algorithm, a lot of papers investigate the discrimination among different fault types based on voltage and current signals, such as ITSC and PD, [115,131,135,200,201], eccentricity and PD [198,200,202,203], etc.

Since demagnetization of PM is sensitive to temperature, the influence of PD on machine temperature is analyzed in [204], and the temperature of the shell and winding are used in addition to current, torque, and speed signals.

 doi:10.20944/preprints202412.1988.v1

3.4.2. Magnetic Signals

In [205–207], airgap flux density is measured with three gauss meter probes located in different position in airgap of a double side linear PMSM. In [205], complex CWT and Teager-Kaiser energy operator are used to extract the fault feature, while in [206], time-time-transform is used. Random forest and extreme learning machine are adopted as classifier respectively. Other than using flux density measuring sensors, search coils wound on tooth [136] and yoke [208] are also adopted to capture the distortion in airgap flux density.

In [209], stray flux signal sampled outside the stator back-iron is converted into symmetric dot pattern image and analysed by wavelet scattering convolution network and semi-supervised deep rule-based classifier. Similar stray flux sensors are placed in [210], while the sampled signals are processed with the local outlier filter and deep Q-network.

3.4.3. Comparison

Table 6 concludes the general advantages and disadvantages of different kinds of data-based methods discussed in this section.

Table 6. Comparison among data-based methods of PD detection.

Signal Sources		Advantages		Disadvantages	
Electrical signals	Voltages & currents	+ Non-invasive	+ Suitable for multi-sensors fusion + High sensitivity	- Influenced by machine topology	- High computational burden
Magnetic signals	Airgap flux	+ Universal		- Need extra sensors	
	Stray flux	+ Less invasive			
Others	Torque	+ Non-invasive			
	Acoustic noise				

4. Eccentricity Detection

4.1. Background

Eccentricity refers to the misalignment of the geometrical center of rotor and stator, resulting in an unevenly distributed airgap. Many factors can cause eccentricity, such as manufacture tolerance, bearing faults, rotor deformation, etc. Generally, there are 3 types of eccentricity, including static eccentricity (SE), dynamic eccentricity (DE), and mix eccentricity (ME).

SE occurs when the rotating center of rotor is not aligned with the center of stator O_s, while being aligned with the geometric center of rotor O_r. As shown in Figure 13 (a), SE results in an unevenly distributed but time-invariant airgap.

On the other hand, DE means the rotating center of rotor is aligned with the center of stator O_s but misaligned with the geometric center of rotor O_r. It can be seen from Figure 13 (b) that the position of minimum airgap rotates with rotor, but the average airgap length is still the nominal airgap length.

ME is essentially the mixture of SE and DE.

With an uneven airgap, eccentricity causes harmonics in back-EMF [211] and currents, torque ripple, the unbalanced magnetic pull (UMP) [212], and vibration [213]. It is also reported in [214] that eccentricity has very significant influence on cogging torque in machines having $2p=N_s\pm1$, where p is the pole-pair number and N_s is the number of stator slots.

Preprints.org (www.preprints.org) | NOT PEER-REVIEWED | Posted: 24 December 2024 doi:10.20944/preprints202412.1988.v1

(a) (b)

Figure 13. Illustration of eccentricity. (a) SE; (b) DE.

4.2. Signal-Based Methods

Classification of signal-based methods for eccentricity detection is shown in Figure 14.

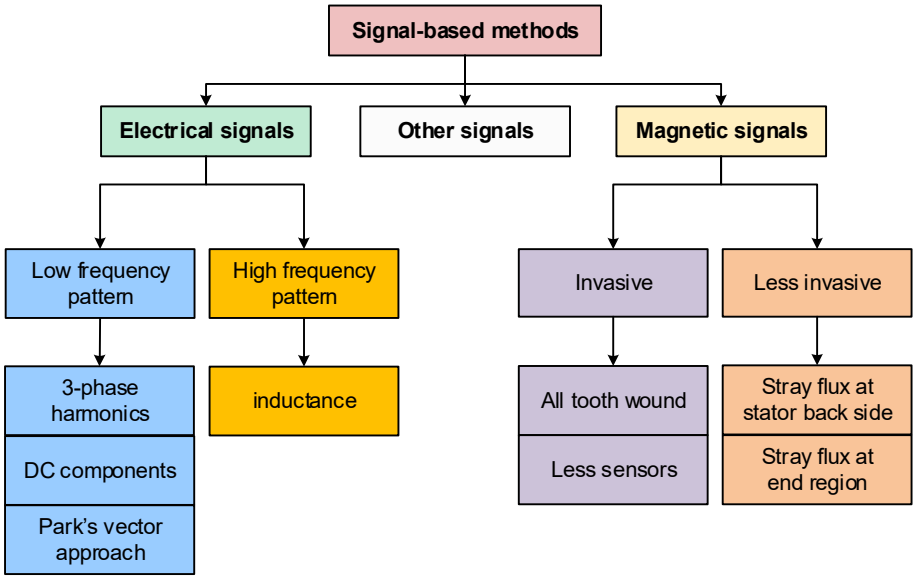

Figure 14. Classification of signal-based methods for eccentricity detection.

4.2.1. Electrical Signals

a) LF pattern

Fractional harmonics are commonly observed in stator currents and voltages when eccentricity fault occurs. The harmonics caused by DE can be expressed as (2) [147,215]:

$$f_{de} = f_e\left(1 \pm \frac{2k-1}{p}\right), k = 1,2,3,\cdots. \quad (2)$$

Meanwhile, the $(1+2k/p)^{th}$ harmonics are found related to SE in [215] for the studied machine.

For DE detection, the 2/3rd and 4/3rd harmonics of a 6-poles BLDC are analysed and tracked with windowed Fourier transform [216], analytical wavelet transform [217], and quadratic time-frequency representation methods [218]. Meanwhile, frequency components with even multiple of mechanical frequency harmonics are selected as fault indicator for DE in [26], and found able to distinguish DE from ITSC faults. Discrimination of DE from PD is accomplished in [219] based on the amplitudes and phase angles of monitored harmonics. IPMSMs and SPMSMs are compared in [220] and found no impact on the harmonics existence. Similar frequency components are obtained in [221] through synchronous resampling to get better consistency at various operation conditions.

For SE detection, the $1/4^{th}$ harmonics is selected of a 9-slot 8-poleSPMSM in [155]. Skarmoutsos *et al*. [222] propose an algorithm to analytically calculate the fractional harmonics that exist in phase voltage and point out that the coil and pole number can influence the harmonic existence expressed

 doi:10.20944/preprints202412.1988.v1

in (2). It is also discovered in [211] the back-EMF is not affected by eccentricity in rotational symmetrical machines, leading to a reduction in fault harmonics.

Integer harmonics also emerge when eccentricity fault occurs. In [188], the NSC of the 7^{th} harmonic in currents is chosen as fault indicator for SE. The fundamental frequency component in ZSVC difference between two sets of windings in a DTPPMSM is used for SE detection in [223], while the sideband $(1\pm1/p)^{th}$ harmonics are used for DE detection.

As mentioned in the methods of ITSC and PD faults, the variation of fundamental frequency components are used in [42] to discriminate ITSC, PD, and SE. Back-EMF at various speed and speed-fluctuation conditions is collected and used for DE detection in [224].

b) HF pattern

HF pattern can reflect the changes of inductance due to the fault. It is pointed out that variation in PM flux results in the saturation degree in *d*-axis, and thus, changes the *d*-axis inductance [225]. A pulsating voltage at *d*-axis is injected at standstill condition to calculate the *d*-axis inductance, and consequently detect SE. The method is further extended [160] to non-standstill conditions and enabled to discriminate demagnetization and DE. A DC voltage in *d*-axis is further injected superimposed with a pulsating HF voltage, and incremental inductance is calculated with the response current. The increase and decrease of inductance compared with healthy machine are used as features for demagnetization and eccentricity faults. Furthermore, Liu *et al*. [191] utilize the mechanical frequency fluctuation of *d*-axis inductance to detect DE. Similarly, Aggarwal *et al*. [226] propose an off-line test method based on incremental inductance, while another criterion is added, that is the hump height of inductance curve versus current.

4.2.2. Magnetic Signals

Similar to the PD fault, the eccentricity fault features may be influenced by the machine topology [211,222]. In comparison, the magnetic signals directly monitor the field distribution, while without relying on the signals filtered by the phase windings. Thus, magnetic signals have a significant advantage of universality in the detection of eccentricity.

a) Invasive methods

Search coils wound on each tooth are feasible to detect both SE and DE, and also able to distinguish them from each other [71,165,170]. In [165], two specially designed fault indicators are calculated from the induced voltages to separately distinguish PD and eccentricity faults. Meanwhile, the nominal peak values of the induced voltages are used as fault indicators in [170]. Furthermore, only one search coil in [227] is placed in slots, whose coil pitch is about the even number of pole-pitch to eliminate induced voltage at healthy condition. In [228], Hall sensors are placed at the slot opening. The NSC and the single-side-band components in flux density are used as fault signatures of SE and DE, respectively.

b) Less invasive methods

Sensors are mounted onto the stator back side of a synchronous generator to capture the stray field [229,230] and manage to distinguish SE and DE. An analytical method is developed in [231] to predict the stray flux at the stator back side at SE condition. Hall sensors are mounted at the end region in [182,232] to capture the distortion due to eccentricity. In [232], the RMS of induced voltages is compared among the four search coils. It is proved that digital Hall sensor is also feasible as a cheaper alternative of analog Hall sensor [182].

4.2.3. Other Signals

Cogging torque is found to contain signatures of eccentricity in [233,234]. It is also stated in [235] by measuring the UMP, discrimination can be achieved between SE and DE. Furthermore, the vibration and acoustic noise caused by eccentricity is investigated in [236] and [237], respectively.

In [238], the temperature asymmetry of the whole machine is utilized for SE detection. The asymmetry in iron loss distribution is discovered when SE exists, resulting in the asymmetry of temperature.

 doi:10.20944/preprints202412.1988.v1

4.2.4. Comparison

Table 7 concludes the general advantages and disadvantages of different kinds of signal-based methods discussed in this section.

Table 7. Comparison among signal-based methods of eccentricity detection.

Fault Signature Types			Advantages	Disadvantages
Electrical signals		Voltage/Current spectrum	+ Non-invasive	- Dependent on winding topology / machine topology
		Impedance	+ Less influenced by machine topology	- Highly sensitive to working conditions
Magnetic signals	Invasive	All tooth wound	+ High sensitivity	- Need a lot of sensors - Invasive
		Fewer sensors	+ Relatively low cost	
	Less invasive	Stator back side	+ Less invasive	- Influenced by housing - Need accurate position of search coils
		End region		

4.3. Model-Based Methods

According to the criteria adopted in this paper, very few methods for eccentricity detection are classified as model-based methods. Thus, this category of methods is omitted here.

4.4. Data-Based Methods

Classification of data-based methods for eccentricity detection is shown in Figure 15.

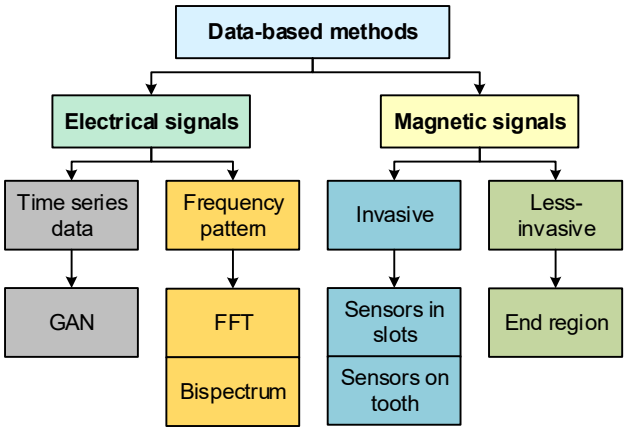

Figure 15. Classification of data-based methods for eccentricity detection.

4.4.1. Electrical Signals

Ebrahimi *et al*. [215] extract the sideband frequency components from stator currents, and KNN classifier is cascaded with an artificial neural network (ANN) to distinguish SE, DE and ME. Furthermore in [239], the fault features of SE and DE are extracted from the harmonics around the fundamental frequency component and classified with SVM. Similar harmonics are used in [240], while the harmonics are obtained with wavelet analysis. The classification is achieved with KNN, and the evaluation of severity is achieved with SVM. In [198], three phase currents are processed with Bispectrum analysis and converted into images. Specifically, the information in different frequency

 doi:10.20944/preprints202412.1988.v1

ranges is separately extracted and transformed into images to minimize the invalid information for ME detection.

In [200], the time and frequency indices are calculated with *dq* currents and fed into different outlier detection methods, including Isolation Forest, SVM, and Robust Covariance Ellipse. The results of these methods are ensembled by Majority Voting Ensemble techniques.

The eccentricity fault in DTPPMSM is analysed in [203]. The voltage angle increases at SE conditions compared with healthy conditions. Thus, the voltage angle is then processed with multivariate regression analysis and ANNs for fault classification.

A method is proposed in [241] using generative adversarial network (GAN) to solve the problem of data lacking for data-based eccentricity detection methods. GAN is employed to generate back-EMF data similar to the actual data, based on the data calculated from the analytical model. Furthermore, in [242], a new fault diagnosis framework is proposed where only healthy data is required. The GAN is used to combine the data provided by ideal mathematical and FEM model of PMSM with eccentricity and the actual data, and eventually provides accurate prediction of back-EMF at different eccentricity degrees.

4.4.2. Magnetic Signals

In [136], the ITSC, PD, SE, and DE can be successfully detected and separated based on the search coils wound on tooth. The SqueezeNet is adopted to capture those fault features in the induced voltages that can distinguish these faults from each other.

In [202], six search coils placed in slots are used as the signal sources, and the amplitudes of the fractional harmonics in the induced voltage are classified based on Random Forest, achieving an accurate detection of DE and discrimination from PD.

In [243], the stray flux in the end region of a linear PMSM is collected with TMR sensors. Gramian Angular Field and Markov Transition Field are used to convert 1-D data into 2-D images, which is then processed with fusion feature extraction algorithms and neural networks.

4.4.3. Comparison

Table 8 concludes the general advantages and disadvantages of different kinds of data-based methods discussed in this section.

Table 8. Comparison among data-based methods of eccentricity detection.

Fault Signature Types			Advantages	Disadvantages
Electrical signals			+ Non-invasive	- Dependent on winding topology / machine topology
Magnetic signals	Invasive	All tooth wound	+ High sensitivity + Able to distinguish SE, DE, PD, and ITSC	- Need a lot of sensors - Invasive
		Fewer sensors	+ Relatively low cost + Able to distinguish DE from PD	- Invasive
	Less invasive	End region	+ Less invasive	- Low SNR

5. Discussion of Detection of Three Types of Faults

5.1. Signal-Based Methods

The ITSC, PD, SE, and DE all introduce unwanted harmonics in currents but with different frequencies. However, the PD, SE, and DE fault-related harmonics are much more sensitive to the machine topology compared to the ITSC fault. This is because the windings act as filters to the harmonics introduced by rotor faults. In contrast, it is more difficult for the windings to filter through

 doi:10.20944/preprints202412.1988.v1

the harmonics caused by the faults in themselves. Consequently, it can be observed that magnetic signals have higher SNR and better universality for rotor faults detection.

5.2. Model-Based Methods

The model-based methods are much more popular in the area of ITSC fault detection than the other two. This could be due to the phenomenon stated before, that is, in some cases the information in the stator currents and voltages are not enough.

5.3. Data-Based Methods

Data-based methods have gained more and more attention in recent years. It can be observed that the recent trend in data-based methods is integrating multiple types of signals, i.e., sensor fusion, and distinguishing different kinds of faults. These tasks are very difficult for traditional techniques due to the highly non-linear and uncertain relationship between the fault signatures and the faults, especially in practical applications. However, since machine learning algorithms, especially those deep learning algorithms, have very strong representation capability, this relationship can possibly be learnt with enough data and appropriate algorithms.

6. Conclusion and Future Work

The state-of-the-art techniques of fault detection methods of PMSMs are comprehensively reviewed in this paper. Three major faults are covered, i.e., the ITSC fault, the PD fault, and the eccentricity fault. The existing methods are classified into signal-, model-, and data-based methods, and further categorized according to the signal types they used. Then, the existing methods are discussed in detail, and special attention is paid to the fault signatures they use. Subsequently, comparison is conducted between methods with different signal sources and fault signatures, as well as the methods for three types of faults. Generally speaking, signal-based methods are relatively simple and low computational burden, while difficult to suppress transient false alarm. Model-based methods are more suitable for transient working conditions, but at the cost of higher computational burden and lower SNR. Data-based methods are the hottest topic in recent years. They have advantages of high SNR and strong capability of distinguishing different faults. But the computational burden is usually very high.

According to the discussions and analyses in this paper, future research can be initiated in the following directions:

(1) Improving the capability of distinguishing different faults. It has been widely investigated how to distinguish different faults, while very few methods with good universality are developed.
(2) Reduction in the number of sensors. Much effort has been made to reduce the number of sensors used for magnetic signal and ZSVC collection. Further investigation can follow this direction and try to find a balance point between the detection capability and complexity.
(3) Detection of faults in DTPPMSM. Compared with traditional three phase PMSM, DTPPMSM has more control degrees, and also more sampled current signals. Thus, potentially higher SNR can be achieved.

Author Contributions: Conceptualization, Z.Q.Z. and H.L.; Methodology, Z.Q.Z. and H.L.; Formal Analysis, H.L.; Investigation, H.L.; Resources, Z.Q.Z.; Writing—Original Draft Preparation, H.L.; Writing—Review & Editing, Z.Q.Z., Z.A., R.C., and Z.Y.W.; Supervision, Z.Q.Z., Z.A. R.C., Z.Y.W.; Project Administration, Z.Q.Z.; Funding Acquisition, Z.Q.Z. and Z.A. All authors have read and agreed to the published version of the manuscript.

Funding: This work was supported by the Siemens Gamesa Renewable Energy A/S, Denmark, under Grant No. R/173973-11-1.

Data Availability Statement: Not applicable.

Conflicts of Interest: The authors declare that they have no conflicts of interest. The funder had no role in the design of the study; in the collection, analyses, or interpretation of data, in the writing of the manuscript; or in the decision to publish the results.

 doi:10.20944/preprints202412.1988.v1

Acronyms

AI	Artificial intelligence
ANN	Artificial neural network
BLDC	Brushless DC
CNN	Convolutional neural network
CWT	Continuous wavelet transform
DE	Dynamic eccentricity
DTPPMSM	Dual-three-phase PMSM
DWT	Discrete wavelet transform
EMD	Empirical mode decomposition
EMF	Electromotive force
EPVA	Extended Park's vector approach
FEM	Finite element method
FFT	Fast Fourier transform
GAN	Generative adversarial network
HF	High frequency
HRC	High resistance connection
IPMSM	Interior PMSM
IRP	Instantaneous reactive power
ITSC	Inter-turn short-circuit
KNN	K-Nearest Neighbor
LF	Low frequency
LUT	Look-up table
MCSA	Machine current signature analysis
ME	Mixed eccentricity
MMF	Magnetomotive force
NSC	Negative sequence component
PD	Partial demagnetization
PLL	Phase lock loop
PM	Permanent magnet
PMSG	PM synchronous generator
PMSM	PM synchronous machine
PSC	Positive sequence component
PVA	Park's vector approach
PWM	Pulse width modulation
RMS	Root mean square
RNN	Recurrent neural network
SE	Static eccentricity
SNR	Signal-to-noise ratio
SPMSM	Surface-mounted PMSM
STFT	Short-time Fourier transform
SVPWM	Space vector PWM
TMR	Tunnelling magneto-resistive
UD	Uniform demagnetization
UMP	Unbalanced magnetic pull
VMD	Variational mode decomposition
ZSC	Zero sequence component
ZSVC	Zero sequence voltage component

References

1. Zhu, Z.Q.; Howe, D. Electrical Machines and Drives for Electric, Hybrid, and Fuel Cell Vehicles. *Proc. IEEE* **2007**, *95*, 746–765. https://doi.org/10.1109/JPROC.2006.892482.
2. Zhang, P.; Du, Y.; Habetler, T.G.; Lu, B. A Survey of Condition Monitoring and Protection Methods for Medium-Voltage Induction Motors. *IEEE Trans. Ind. Appl.* **2011**, *47*, 34–46. https://doi.org/10.1109/tia.2010.2090839.
3. Orlowska-Kowalska, T.; Wolkiewicz, M.; Pietrzak, P.; Skowron, M.; Ewert, P.; Tarchala, G.; Krzysztofiak, M.; Kowalski, C.T. Fault Diagnosis and Fault-Tolerant Control of PMSM Drives–State of the Art and Future Challenges. *IEEE Access* **2022**, *10*, 59979–60024. https://doi.org/10.1109/access.2022.3180153.
4. Pengbo, Z.; Renxiang, C.; Xiangyang, X.; Lixia, Y.; Mengyu, R. Recent Progress and Prospective Evaluation of Fault Diagnosis Strategies for Electrified Drive Powertrains: A Comprehensive Review. *Measurement* **2023**, *222*, 113711. https://doi.org/10.1016/j.measurement.2023.113711.
5. Jiang, Y.; Ji, B.; Zhang, J.; Yan, J.; Li, W. An Overview of Diagnosis Methods of Stator Winding Inter-Turn Short Faults in Permanent-Magnet Synchronous Motors for Electric Vehicles. *WEVJ* **2024**, *15*, 165. https://doi.org/10.3390/wevj15040165.
6. Faiz, J.; Bazrafshan, M.A.; Tabarniarami, Z. Demagnetisation Fault Analysis and Diagnosis Based on Different Methods in Permanent Magnet Machines-An Overview. *IET Electric Power Applications* **2024**.
7. Faiz, J.; Nejadi-Koti, H. Eccentricity Fault Diagnosis Indices for Permanent Magnet Machines: State-of-the-art. *IET Electric Power Applications* **2019**, *13*, 1241–1254. https://doi.org/10.1049/iet-epa.2018.5751.
8. Solís, R.; Torres, L.; Pérez, P. Review of Methods for Diagnosing Faults in the Stators of BLDC Motors. *Processes* **2022**, *11*. https://doi.org/10.3390/pr11010082.
9. Grubic, S.; Aller, J.M.; Bin, L.; Habetler, T.G. A Survey on Testing and Monitoring Methods for Stator Insulation Systems of Low-Voltage Induction Machines Focusing on Turn Insulation Problems. *IEEE Trans. Ind. Electron.* **2008**, *55*, 4127–4136. https://doi.org/10.1109/tie.2008.2004665.
10. Hang, J.; Zhang, J.; Cheng, M.; Huang, J. Online Interturn Fault Diagnosis of Permanent Magnet Synchronous Machine Using Zero-Sequence Components. *IEEE Trans. Power Electron.* **2015**, *30*, 6731–6741. https://doi.org/10.1109/tpel.2015.2388493.
11. Zhu, Y.; Cai, S.; Li, B. Detection and Discrimination of Interturn Fault and High-Resistance Connection Fault in PMSM Based on Deviation Angle of Zero Sequence Voltage. *IEEE Trans. Transp. Electrific.* **2024**, *10*, 7623–7632. https://doi.org/10.1109/TTE.2023.3344711.
12. Hang, J.; Ding, S.; Ren, X.; Hu, Q.; Huang, Y.; Hua, W.; Wang, Q. Integration of Interturn Fault Diagnosis and Torque Ripple Minimization Control for Direct-Torque-Controlled SPMSM Drive System. *IEEE Trans. Power Electron.* **2021**, *36*, 11124–11134. https://doi.org/10.1109/tpel.2021.3073774.
13. Hang, J.; Sun, W.; Hu, Q.; Ren, X.; Ding, S. Integration of Interturn Fault Diagnosis and Fault-Tolerant Control for PMSM Drive System. *IEEE Trans. Transp. Electrif.* **2022**, *8*, 2825–2835. https://doi.org/10.1109/tte.2021.3134821.
14. Wang, H.; Wang, J.; Wang, X.; Lu, S.; Hu, C.; Cao, W. Detection and Evaluation of the Interturn Short Circuit Fault in a BLDC-Based Hub Motor. *IEEE Trans. Ind. Electron.* **2023**, *70*, 3055–3068. https://doi.org/10.1109/tie.2022.3167167.
15. Laadjal, K.; Antunes, H.R.P.; Sahraoui, M.; Bento, F.; Marques Cardoso, A.J. On-Line Diagnosis and Discrimination of Stator Faults in Six-Phase Induction Motors, Based on Voltage Symmetrical Components. *IEEE Trans. Transp. Electrif.* **2022**, 1–1. https://doi.org/10.1109/tte.2022.3219722.
16. Laadjal, K.; Bento, F.; Serra, J.; Cardoso, A.J.M. An Integrated Strategy for the Real-Time Detection and Discrimination of Stator Inter-Turn Short-Circuits and Converter Faults in Asymmetrical Six-Phase Induction Motors. *IEEE Trans. on Ind. Applicat.* **2023**, 1–10. https://doi.org/10.1109/TIA.2023.3321266.
17. Alloui, A.; Laadjal, K.; Sahraoui, M.; Marques Cardoso, A.J. Online Interturn Short-Circuit Fault Diagnosis in Induction Motors Operating Under Unbalanced Supply Voltage and Load Variations, Using the STLSP Technique. *IEEE Trans. Ind. Electron.* **2023**, *70*, 3080–3089. https://doi.org/10.1109/TIE.2022.3172751.

18. Wu, Y.; Zhang, J.; Xu, Z.; Wang, S.; Fu, H. Feature Extraction and Applicability Comparisons for Fault Detection of Inter-Turn Short-Circuited PMSM. *IEEE Trans. Instrum. Meas.* **2024**, *73*, 1–10. https://doi.org/10.1109/TIM.2024.3415792.
19. Williamson, S.; Mirzoian, K. Analysis of Cage Induction Motors with Stator Winding Faults. *IEEE Trans. on Power Apparatus and Syst.* **1985**, *PAS-104*, 1838–1842. https://doi.org/10.1109/TPAS.1985.319221.
20. Jeong, H.; Moon, S.; Kim, S.W. An Early Stage Interturn Fault Diagnosis of PMSMs by Using Negative-Sequence Components. *IEEE Trans. Ind. Electron.* **2017**, *64*, 5701–5708. https://doi.org/10.1109/tie.2017.2677355.
21. Dorrell, D.G.; Makhoba, K. Detection of Inter-Turn Stator Faults in Induction Motors Using Short-Term Averaging of Forward and Backward Rotating Stator Current Phasors for Fast Prognostics. *IEEE Trans. Magn.* **2017**, *53*, 1–7. https://doi.org/10.1109/tmag.2017.2710181.
22. Ge, Y.; Song, B.; Pei, Y.; Mollet, Y.A.B.; Gyselinck, J.J.C. Analytical Expressions of Isolation Indicators for Permanent-Magnet Synchronous Machines under Stator Short-Circuit Faults. *IEEE Trans. Energy Convers.* **2019**, *34*, 984–992. https://doi.org/10.1109/tec.2018.2878343.
23. Bahloul, I.; Bouzid, M.B.K.; Khil, S.K.E.; Champenois, G. Robust Novel Indicator to Distinguish between an Inter-Turn Short Circuit Fault and Load Unbalance in PMSG. *IEEE Trans. Ind. Appl.* **2023**, 1–9. https://doi.org/10.1109/tia.2023.3236898.
24. Laadjal, K.; Bento, F.; Henriques, K.; Marques Cardoso, A.J.; Sahraoui, M. A Novel Indicator-Based on-Line Diagnostics Technique of Inter-Turn Short-Circuit Faults in Synchronous Reluctance Machines. *IEEE J. Emerg. Sel. Top. Power Electron.* **2023**, 1–1. https://doi.org/10.1109/jestpe.2023.3234339.
25. Naderi, P.; Fathi, A. Fault Diagnosis/Separation of Surface Mounted Permanent Magnet Synchronous Machine by Current and Its Homopolar Orders Analysis. *IEEE Trans. Energy Convers.* **2022**, 1–11. https://doi.org/10.1109/tec.2022.3216686.
26. Park, J.-K.; Hur, J. Detection of Inter-Turn and Dynamic Eccentricity Faults Using Stator Current Frequency Pattern in IPM-Type BLDC Motors. *IEEE Trans. Ind. Electron.* **2016**, *63*, 1771–1780. https://doi.org/10.1109/tie.2015.2499162.
27. Lee, S.-T.; Hur, J. Detection Technique for Stator Inter-Turn Faults in BLDC Motors Based on Third-Harmonic Components of Line Currents. *IEEE Trans. Ind. Appl.* **2017**, *53*, 143–150. https://doi.org/10.1109/tia.2016.2614633.
28. Wang, B.; Wang, J.; Griffo, A.; Sen, B. Stator Turn Fault Detection by Second Harmonic in Instantaneous Power for a Triple-Redundant Fault-Tolerant PM Drive. *IEEE Trans. Ind. Electron.* **2018**, *65*, 7279–7289. https://doi.org/10.1109/tie.2018.2793188.
29. Duan, R.; Wu, L.; Lyu, Z.; Zhan, H.; Song, P. Harmonic Subspace Signature-Based Detection and Localization of Inter-Turn Short Circuit Fault for Dual Three-Phase PMSM with VSD Scheme. *IEEE Trans. Transp. Electrific.* **2024**, 1–1. https://doi.org/10.1109/TTE.2024.3366595.
30. Huang, S.; Aggarwal, A.; Strangas, E.G.; Li, K.; Niu, F.; Huang, X. Robust Stator Winding Fault Detection in PMSMs with Respect to Current Controller Bandwidth. *IEEE Trans. Power Electron.* **2021**, *36*, 5032–5042. https://doi.org/10.1109/tpel.2020.3030036.
31. Rosero, J.A.; Romeral, L.; Ortega, J.A.; Rosero, E. Short-Circuit Detection by Means of Empirical Mode Decomposition and Wigner–Ville Distribution for PMSM Running under Dynamic Condition. *IEEE Trans. Ind. Electron.* **2009**, *56*, 4534–4547. https://doi.org/10.1109/tie.2008.2011580.
32. Dogan, Z.; Tetik, K. Diagnosis of Inter-Turn Faults Based on Fault Harmonic Component Tracking in LSPMSMs Working under Nonstationary Conditions. *IEEE Access* **2021**, *9*, 92101–92112. https://doi.org/10.1109/access.2021.3092605.
33. Chen, C.-S.; Lin, C.-J.; Yang, F.-J.; Lin, F.-C. Model Design of Inter-Turn Short Circuits in Internal Permanent Magnet Synchronous Motors and Application of Wavelet Transform for Fault Diagnosis. *Applied Sciences* **2024**, *14*, 9570. https://doi.org/10.3390/app14209570.
34. Boileau, T.; Leboeuf, N.; Nahid-Mobarakeh, B.; Meibody-Tabar, F. Synchronous Demodulation of Control Voltages for Stator Interturn Fault Detection in PMSM. *IEEE Trans. Power Electron.* **2013**, *28*, 5647–5654. https://doi.org/10.1109/tpel.2013.2254132.

35. Bellini, A.; Filippetti, F.; Franceschini, G.; Tassoni, C. Closed-Loop Control Impact on the Diagnosis of Induction Motors Faults. *IEEE Trans. on Ind. Applicat.* **2000**, *36*, 1318–1329. https://doi.org/10.1109/28.871280.
36. Wei, D.; Liu, K.; Hu, W.; Peng, X.; Chen, Y.; Ding, R. Short-Time Adaline Based Fault Feature Extraction for Inter-Turn Short Circuit Diagnosis of PMSM via Residual Insulation Monitoring. *IEEE Trans. Ind. Electron.* **2023**, *70*, 3103–3114. https://doi.org/10.1109/tie.2022.3167164.
37. Wei, D.; Liu, K.; Huang, J.; Wang, J.; Zhou, S.; Cai, H.; Chen, J. Instantaneous Phase Estimation Based Single-Signal Diagnosis for Inter-Turn Short Circuit Fault in PMSMs. *IEEE Trans. Energy Convers.* **2024**, 1–15. https://doi.org/10.1109/TEC.2024.3480971.
38. Ghods, M.; Tabarniarami, Z.; Faiz, J.; Bazrafshan, M.A. Turn-to-Turn and Phase-to-Phase Short Circuit Fault Detection of Wind Turbine Permanent Magnet Generator Based on Equivalent Magnetic Network Modelling by Wavelet Transform Approach. *IET Electric Power Applications* **2024**, *18*, 1005–1020. https://doi.org/10.1049/elp2.12452.
39. Niu, F.; Xu, M.; Zhou, F.; Huang, S.; Xu, Z.; Zhang, L.; Aggarwal, A. Accurate Interturn Short-Circuit Faults Diagnosis in PMSMs under Variable Operating Conditions by Signal Compensation. *IEEE Trans. Power Electron.* **2024**, 1–13. https://doi.org/10.1109/TPEL.2024.3487628.
40. Fonseca, D.S.B.; Santos, C.M.C.; Cardoso, A.J.M. Stator Faults Modeling and Diagnostics of Line-Start Permanent Magnet Synchronous Motors. *IEEE Trans. Ind. Appl.* **2020**, *56*, 2590–2599. https://doi.org/10.1109/tia.2020.2979674.
41. Qiao, J.; Yin, X.; Wang, Y.; Lu, Q.; Tan, L.; Zhu, L. A Stator Internal Short-Circuit Fault Protection Method for Turbo-Generator Based on Instantaneous Power Oscillation Ratio. *IEEE Trans. Energy Convers.* **2023**, 1–9. https://doi.org/10.1109/tec.2023.3237217.
42. Haddad, R.Z.; Lopez, C.A.; Foster, S.N.; Strangas, E.G. A Voltage-Based Approach for Fault Detection and Separation in Permanent Magnet Synchronous Machines. *IEEE Trans. Ind. Appl.* **2017**, *53*, 5305–5314. https://doi.org/10.1109/tia.2017.2726072.
43. Moon, S.; Jeong, H.; Lee, H.; Kim, S.W. Detection and Classification of Demagnetization and Interturn Short Faults of IPMSMs. *IEEE Trans. Ind. Electron.* **2017**, *64*, 9433–9441. https://doi.org/10.1109/tie.2017.2703919.
44. Ullah, Z.; Lee, S.-T.; Hur, J. A Torque Angle-Based Fault Detection and Identification Technique for IPMSM. *IEEE Trans. Ind. Appl.* **2020**, *56*, 170–182. https://doi.org/10.1109/tia.2019.2947401.
45. Tabarniarami, Z.; Ghods, M.; Faiz, J.; Abedini, M. Online Diagnosis of Short Circuit Faults of Permanent Magnet Synchronous Generator by Short-Time Analysis of the Three Phase Amplitude-Phase Signal Based on Analytical Modeling. *IEEE Trans. Transp. Electrific.* **2024**, 1–1. https://doi.org/10.1109/TTE.2024.3369970.
46. Hang, J.; Wang, X.; Li, W.; Ding, S. Interturn Short-Circuit Fault Diagnosis and Fault-Tolerant Control of DTP-PMSM Based on Subspace Current Residuals. *IEEE Trans. Power Electron.* **2024**, 1–9. https://doi.org/10.1109/TPEL.2024.3484469.
47. Wang, H.; Hu, J.; Li, Y. Fault Phase Location for Interturn Short Circuit Faults in Symmetrical Six-Phase PMSMs Based on Subspace Current Residual. *IEEE Trans. Transp. Electrific.* **2024**, 1–1. https://doi.org/10.1109/TTE.2024.3358626.
48. Hu, J.; Wang, H.; Li, Y. Model-Based Severity Monitoring for Interturn Short Circuit Faults in Symmetrical Six-Phase PMSMs Using Subspace Current Residuals. *IEEE Trans. Power Electron.* **2023**, *38*, 16142–16152. https://doi.org/10.1109/TPEL.2023.3314652.
49. Sen, B.; Wang, J. Stator Interturn Fault Detection in Permanent-Magnet Machines Using PWM Ripple Current Measurement. *IEEE Trans. Ind. Electron.* **2016**, *63*, 3148–3157. https://doi.org/10.1109/tie.2016.2515560.
50. Wang, B.; Hu, J.; Wang, G.; Hua, W. A Novel Stator Turn Fault Detection Technique by Using Equivalent High Frequency Impedance. *IEEE Access* **2020**, *8*, 130540–130550. https://doi.org/10.1109/access.2020.3009109.
51. Hu, R.; Wang, J.; Sen, B.; Mills, A.R.; Chong, E.; Sun, Z. PWM Ripple Currents Based Turn Fault Detection for Multiphase Permanent Magnet Machines. *IEEE Trans. Ind. Appl.* **2017**, *53*, 2740–2751. https://doi.org/10.1109/tia.2016.2642193.

52. Hu, R.; Wang, J.; Mills, A.; Chong, E.; Sun, Z. Detection and Classification of Turn Fault and High-resistance Connection Fault in Inverter-fed Permanent Magnet Machines Based on High-frequency Signals. *J. Eng.* **2019**, *2019*, 4278–4282. https://doi.org/10.1049/joe.2018.8253.
53. Hu, R.; Wang, J.; Mills, A.R.; Chong, E.; Sun, Z. Detection and Classification of Turn Fault and High Resistance Connection Fault in Permanent Magnet Machines Based on Zero Sequence Voltage. *IEEE Trans. Power Electron.* **2020**, *35*, 1922–1933. https://doi.org/10.1109/tpel.2019.2922114.
54. Gao, F.; Zhang, G.; Li, M.; Gao, Y.; Zhuang, S. Inter-Turn Fault Identification of Surface-Mounted Permanent Magnet Synchronous Motor Based on Inverter Harmonics. *Energies* **2020**, *13*. https://doi.org/10.3390/en13040899.
55. Wang, B.; Luo, L.; Fu, W.; Hua, W.; Wang, G.; Wang, Z. Study on the PWM Ripple Current Based Turn Fault Detection for Interior PM Machine. *IEEE Trans. Transp. Electrif.* **2021**, *7*, 1537–1547. https://doi.org/10.1109/tte.2021.3050560.
56. Zhang, J.; Xu, Z.; Wang, J.; Zhao, J.; Din, Z.; Cheng, M. Detection and Discrimination of Incipient Stator Faults for Inverter-Fed Permanent Magnet Synchronous Machines. *IEEE Trans. Ind. Electron.* **2021**, *68*, 7505–7515. https://doi.org/10.1109/tie.2020.3009563.
57. Xu, Z.; Zhang, J.; Zhang, Y.; Zhao, J. Winding Condition Monitoring for Inverter-Fed PMSM Using High-Frequency Current Injection. *IEEE Trans. Ind. Appl.* **2021**, *57*, 5818–5828. https://doi.org/10.1109/tia.2021.3103923.
58. Hu, R.; Wang, J.; Mills, A.R.; Chong, E.; Sun, Z. High-Frequency Voltage Injection Based Stator Interturn Fault Detection in Permanent Magnet Machines. *IEEE Trans. Power Electron.* **2021**, *36*, 785–794. https://doi.org/10.1109/tpel.2020.3005757.
59. Wang, H.; Wu, Z.; Zhou, F.; Cao, W.; Hu, C.; Lu, S. Diagnosis of Interturn Short Circuit Fault in BLDCM Based on Coupled High-Frequency Signal Injection. *IEEE Trans. Instrum. Meas.* **2024**, *73*, 1–10. https://doi.org/10.1109/TIM.2024.3457950.
60. Xu, Z.; Zhang, J.; Cheng, M. Investigation of Signal Injection Methods for Fault Detection of PMSM Drives. *IEEE Trans. Energy Convers.* **2022**, 1–1. https://doi.org/10.1109/tec.2022.3168690.
61. Xu, Z.; Zhang, J.; Xiong, J.; Wu, Y.; Cheng, M. An Improved High Frequency Voltage Injection Method for Inter-Turn Short-Circuit Fault Detection in PMSMs. *IEEE Trans. Transp. Electrif.* **2022**, 1–1. https://doi.org/10.1109/tte.2022.3225686.
62. Fang, X.; Gao, J.; Lu, J.; Zhang, J.; Li, H. Early Fault Detection of Stator Inter-Turn Short Circuit of Asynchronous Motor Based on Rotating High Frequency Voltage Injection. *IEEE Trans. Transp. Electrific.* **2024**, 1–1. https://doi.org/10.1109/TTE.2024.3439727.
63. Qi, Y.; Zafarani, M.; Akin, B.; Fedigan, S.E. Analysis and Detection of Inter-Turn Short-Circuit Fault through Extended Self-Commissioning. *IEEE Trans. Ind. Appl.* **2017**, *53*, 2730–2739. https://doi.org/10.1109/tia.2016.2626264.
64. Baruti, K.H.; Gurusamy, V.; Erturk, F.; Akin, B. A Robust and Practical Approach to Estimate the Number of Shorted Turns in PMSM with ITSC Faults. *IEEE J. Emerg. Sel. Top. Power Electron.* **2021**, *9*, 2839–2849. https://doi.org/10.1109/jestpe.2020.3011692.
65. Hang, J.; Ding, S.; Zhang, J.; Cheng, M.; Chen, W.; Wang, Q. Detection of Interturn Short-Circuit Fault for PMSM with Simple Fault Indicator. *IEEE Trans. Energy Convers.* **2016**, *31*, 1697–1699. https://doi.org/10.1109/tec.2016.2583780.
66. Haje Obeid, N.; Battiston, A.; Boileau, T.; Nahid-Mobarakeh, B. Early Intermittent Interturn Fault Detection and Localization for a Permanent Magnet Synchronous Motor of Electrical Vehicles Using Wavelet Transform. *IEEE Trans. Transp. Electrif.* **2017**, *3*, 694–702. https://doi.org/10.1109/tte.2017.2743419.
67. Hang, J.; Zhang, J.; Xia, M.; Ding, S.; Hua, W. Interturn Fault Diagnosis for Model-Predictive-Controlled-PMSM Based on Cost Function and Wavelet Transform. *IEEE Trans. Power Electron.* **2020**, *35*, 6405–6418. https://doi.org/10.1109/tpel.2019.2953269.
68. Ray, D.K.; Roy, T.; Chattopadhyay, S. Skewness Scanning for Diagnosis of a Small Inter-Turn Fault in Quadcopter's Motor Based on Motor Current Signature Analysis. *IEEE Sens. J.* **2021**, *21*, 6952–6961. https://doi.org/10.1109/jsen.2020.3038786.

69. Park, C.H.; Lee, J.; Kim, H.; Suh, C.; Youn, M.; Shin, Y.; Ahn, S.-H.; Youn, B.D. Drive-Tolerant Current Residual Variance (DTCRV) for Fault Detection of a Permanent Magnet Synchronous Motor under Operational Speed and Load Torque Conditions. *IEEE Access* **2021**, *9*, 49055–49068. https://doi.org/10.1109/access.2021.3068425.
70. Jafari, A.; Faiz, J.; Jarrahi, M.A. A Simple and Efficient Current-Based Method for Interturn Fault Detection in BLDC Motors. *IEEE Trans. Ind. Inform.* **2021**, *17*, 2707–2715. https://doi.org/10.1109/tii.2020.3009867.
71. Da, Y.; Shi, X.; Krishnamurthy, M. A New Approach to Fault Diagnostics for Permanent Magnet Synchronous Machines Using Electromagnetic Signature Analysis. *IEEE Trans. Power Electron.* **2013**, *28*, 4104–4112. https://doi.org/10.1109/tpel.2012.2227808.
72. Huang, W.; Du, B.; Li, T.; Sun, Y.; Cheng, Y.; Cui, S. Interturn Short-Circuit Fault Diagnosis of Interior Permanent Magnet Synchronous Motor for Electric Vehicle Based on Search Coil. *IEEE Trans. Power Electron.* **2023**, *38*, 2506–2515. https://doi.org/10.1109/tpel.2022.3213512.
73. Gao, C.; Miao, Z.; Sang, X.; Xu, X.; Si, J.; Alkahtani, M. A Multi-Faults Online Detection and Identification Method for Concentrated Winding PMSM Using Search Coil Array. *IEEE Trans. Transp. Electrific.* **2024**, 1–1. https://doi.org/10.1109/TTE.2024.3446594.
74. Mühlthaler, J.; Lehner, B.; Reeh, A. Detection of Inter-Turn Short-Circuits in Permanent Magnet Machines Based on Rogowski & Search Coil Based Monitoring. In Proceedings of the 2024 International Conference on Electrical Machines (ICEM); IEEE: Torino, Italy, September 1 2024; pp. 1–8.
75. Zeng, C.; Huang, S.; Yang, Y.; Wu, D. Inter-turn Fault Diagnosis of Permanent Magnet Synchronous Machine Based on Tooth Magnetic Flux Analysis. *IET Electr. Power Appl.* **2018**, *12*, 837–844. https://doi.org/10.1049/iet-epa.2017.0865.
76. Li, R.; Fang, H.; Li, D.; Qu, R.; Yang, S.; Wang, R. A Search Coil Design Method of PMSM for Detection of Inter-Turn Short-Circuit Fault. *IEEE Trans. Ind. Electron.* **2023**, 1–10. https://doi.org/10.1109/tie.2023.3274879.
77. Liu, X.; Miao, W.; Xu, Q.; Cao, L.; Liu, C.; Pong, P.W.T. Inter-Turn Short-Circuit Fault Detection Approach for Permanent Magnet Synchronous Machines through Stray Magnetic Field Sensing. *IEEE Sens. J.* **2019**, *19*, 7884–7895. https://doi.org/10.1109/jsen.2019.2918018.
78. Irhoumah, M.; Pusca, R.; Lefevre, E.; Mercier, D.; Romary, R. Detection of the Stator Winding Inter-Turn Faults in Asynchronous and Synchronous Machines through the Correlation between Harmonics of the Voltage of Two Magnetic Flux Sensors. *IEEE Trans. Ind. Appl.* **2019**, *55*, 2682–2689. https://doi.org/10.1109/tia.2019.2899560.
79. Gurusamy, V.; Bostanci, E.; Li, C.; Qi, Y.; Akin, B. A Stray Magnetic Flux-Based Robust Diagnosis Method for Detection and Location of Interturn Short Circuit Fault in PMSM. *IEEE Trans. Instrum. Meas.* **2021**, *70*, 1–11. https://doi.org/10.1109/tim.2020.3013128.
80. Eldeeb, H.H.; Berzoy, A.; Mohammed, O. Stator Fault Detection on DTC-Driven IM via Magnetic Signatures Aided by 2-D FEA Co-Simulation. *IEEE Trans. Magn.* **2019**, *55*, 1–5. https://doi.org/10.1109/tmag.2019.2892707.
81. Assaf, T.; Henao, H.; Capolino, G.A. Simplified Axial Flux Spectrum Method to Detect Incipient Stator Inter-Turn Short-Circuits in Induction Machine.; 2004; pp. 815–819 vol. 2.
82. Lamim Filho, P.C.M.; Rabelo Baccarini, L.M.; Batista, F.B.; Araujo, A.C. Orbit Analysis from a Stray Flux Full Spectrum for Induction Machine Fault Detection. *IEEE Sens. J.* **2021**, *21*, 16152–16161. https://doi.org/10.1109/jsen.2021.3074815.
83. Kumar, P.S.; Xie, L.; Halick, M.S.M.; Vaiyapuri, V. Stator End-Winding Thermal and Magnetic Sensor Arrays for Online Stator Inter-Turn Fault Detection. *IEEE Sens. J.* **2021**, *21*, 5312–5321. https://doi.org/10.1109/jsen.2020.3029041.
84. Bai, W.; Zhou, X.; Wang, Y.; Zeng, Q.; Zhan, S.; Hua, X.; Bao, G. Vibration Analysis of the Electric Drive System with Inter-Turn Short-Circuit and Gear Spalling Faults. *J. Vib. Eng. Technol.* **2023**, *11*, 3595–3605. https://doi.org/10.1007/s42417-022-00770-y.
85. Wu, Y.-H.; Liu, M.-Y.; Song, H.; Li, C.; Yang, X.-L. A Temperature and Magnetic Field-Based Approach for Stator Inter-Turn Fault Detection. *IEEE Sens. J.* **2022**, *22*, 17799–17807. https://doi.org/10.1109/jsen.2022.3198146.

86. Wei, D.; Liu, K.; Zhu, Z.-Q.; Zhou, S.; Wang, J.; Chen, Y. Rotor Speed Signature Analysis-Based Inter-Turn Short Circuit Fault Detection for Permanent Magnet Synchronous Machines. *IET Electric Power Applications* **2024**, *18*, 1187–1199. https://doi.org/10.1049/elp2.12469.
87. Wei, D.; Liu, K.; Wang, J.; Zhou, S.; Cai, H.; Chen, J. Detection of Inter-Turn Short Circuit Fault in Permanent Magnet Synchronous Machine under Phase Current Reconstruction Control. In Proceedings of the 2023 26th International Conference on Electrical Machines and Systems (ICEMS); IEEE: Zhuhai, China, November 5 2023; pp. 2164–2168.
88. Liu, C.; Xiao, L.; Zou, J.; Xu, Y.; Li, S. Analysis and Monitoring Method for Inter-Turn Short-Circuit Fault for PMSM. *IEEE Trans. Magn.* **2023**, *59*, 1–6. https://doi.org/10.1109/TMAG.2023.3294704.
89. Leboeuf, N.; Boileau, T.; Nahid-Mobarakeh, B.; Clerc, G.; Meibody-Tabar, F. Real-Time Detection of Interturn Faults in PM Drives Using Back-EMF Estimation and Residual Analysis. *IEEE Trans. Ind. Appl.* **2011**, *47*, 2402–2412. https://doi.org/10.1109/tia.2011.2168929.
90. Mazzoletti, M.A.; Bossio, G.R.; De Angelo, C.H.; Espinoza-Trejo, D.R. A Model-Based Strategy for Interturn Short-Circuit Fault Diagnosis in PMSM. *IEEE Trans. Ind. Electron.* **2017**, *64*, 7218–7228. https://doi.org/10.1109/tie.2017.2688973.
91. Hu, R.; Wang, J.; Mills, A.R.; Chong, E.; Sun, Z. Current-Residual-Based Stator Interturn Fault Detection in Permanent Magnet Machines. *IEEE Trans. Ind. Electron.* **2021**, *68*, 59–69. https://doi.org/10.1109/tie.2020.2965500.
92. Castro Palavicino, P.; Sarlioglu, B. Estimation of Position and Shorted Turns Percentage of an Inter-Turn Short Circuit in Interior Permanent Magnet Synchronous Machines Based on a Current Observer and Stationary Reference Frame Tracking. *IEEE Trans. on Ind. Applicat.* **2023**, *59*, 4066–4075. https://doi.org/10.1109/TIA.2023.3268996.
93. Mahmoudi, A.; Jlassi, I.; Cardoso, A.J.M.; Yahia, K.; Sahraoui, M. Inter-Turn Short-Circuit Faults Diagnosis in Synchronous Reluctance Machines, Using the Luenberger State Observer and Current's Second-Order Harmonic. *IEEE Trans. Ind. Electron.* **2022**, *69*, 8420–8429. https://doi.org/10.1109/tie.2021.3109514.
94. Qin, Y.; Li, G.J.; Zhu, Z.Q.; Foster, M.P.; Stone, D.A.; Jia, C.J.; McKeever, P. Model-Based Luenberger State Observer for Detecting Interturn Short-Circuits in PM Machines. *IEEE Trans. Transp. Electrific.* **2024**, 1–1. https://doi.org/10.1109/TTE.2024.3478840.
95. Belkhadir, A.; Pusca, R.; Romary, R.; Belkhayat, D.; Zidani, Y. Detection of External Rotor PMSM Inter-Turn Short Circuit Fault Using Extended Kalman Filter. In Proceedings of the 2023 IEEE 14th International Symposium on Diagnostics for Electrical Machines, Power Electronics and Drives (SDEMPED); IEEE: Chania, Greece, August 28 2023; pp. 491–497.
96. Chen, Z.; Liang, D.; Jia, S.; Yang, L.; Yang, S. Incipient Interturn Short-Circuit Fault Diagnosis of Permanent Magnet Synchronous Motors Based on the Data-Driven Digital Twin Model. *IEEE J. Emerg. Sel. Topics Power Electron.* **2023**, *11*, 3514–3524. https://doi.org/10.1109/JESTPE.2023.3255249.
97. Zanuso, G.; Peretti, L. A Voltage-Distortion-Based Method for Robust Detection and Location of Interturn Fault in Permanent Magnet Synchronous Machine. *IEEE Trans. Energy Convers.* **2022**, *38*, 11174–11186. https://doi.org/10.1109/tpel.2022.3167439.
98. Du, B.; Wu, S.; Han, S.; Cui, S. Interturn Fault Diagnosis Strategy for Interior Permanent-Magnet Synchronous Motor of Electric Vehicles Based on Digital Signal Processor. *IEEE Trans. Ind. Electron.* **2016**, *63*, 1694–1706. https://doi.org/10.1109/tie.2015.2496900.
99. Chen, Q.; Han, X.; Liu, G.; Zhao, W.; Shi, H. Inter-Turn Fault Diagnosis and Control for Five-Phase PMSMs by Disturbance Observer. *IEEE Trans. Ind. Electron.* **2024**, 1–9. https://doi.org/10.1109/TIE.2024.3374364.
100. Cui, R.; Fan, Y.; Li, C. On-Line Inter-Turn Short-Circuit Fault Diagnosis and Torque Ripple Minimization Control Strategy Based on OW Five-Phase BFTHE-IPM. *IEEE Trans. Energy Convers.* **2018**, *33*, 2200–2209. https://doi.org/10.1109/tec.2018.2851615.
101. Xu, Y.; Wang, Y.; Zou, J. An Inter-Turn Short-Circuits Fault Detection Strategy Considering Inverter Nonlinearity and Current Measurement Errors for Sensorless Control of SPMSM. *IEEE Trans. Ind. Electron.* **2022**, *69*, 11709–11722. https://doi.org/10.1109/tie.2021.3125653.
102. Upadhyay, A.; Alakula, M. A Theoretical Study of Stator Flux Linkage DC Offset Based Stator Fault Detection for PMSM Drive Systems.; 2022; pp. 1–6.

103. Yang, Y.; Chen, Y.; Hao, W. Online Detection of Inter-turn Short-circuit Fault in Dual-redundancy Permanent Magnet Synchronous Motor. *IET Electr. Power Appl.* **2020**, *15*, 104–113. https://doi.org/10.1049/elp2.12011.
104. Feng, X.; Wang, B.; Liu, C.; Zeng, J.; Wang, Z. Research on Inter-Turn Short-Circuit Fault Diagnosis Method Based on High Frequency Voltage Residual for PMSM. *Trans. Electr. Mach. Syst.* **2023**, *7*, 256–265. https://doi.org/10.30941/CESTEMS.2023.00050.
105. Wang, H.; Hu, J.; Li, Y. Interturn Fault Severity Monitoring in Symmetrical Six-Phase PMSMs Using Subspace Negative-Sequence High-Frequency Current Residuals. *IEEE Trans. Power Electron.* **2024**, 1–10. https://doi.org/10.1109/TPEL.2023.3347662.
106. Fan, P.; Zhang, Y. A Detection Method for Interturn Short-Circuit Fault of Five-Phase Surface Mounted PMSM. In Proceedings of the 2023 26th International Conference on Electrical Machines and Systems (ICEMS); IEEE: Zhuhai, China, November 5 2023; pp. 68–73.
107. Aubert, B.; Regnier, J.; Caux, S.; Alejo, D. Kalman-Filter-Based Indicator for Online Interturn Short Circuits Detection in Permanent-Magnet Synchronous Generators. *IEEE Trans. Ind. Electron.* **2015**, *62*, 1921–1930. https://doi.org/10.1109/tie.2014.2348934.
108. El Sayed, W.; Abd El Geliel, M.; Lotfy, A. Fault Diagnosis of PMSG Stator Inter-Turn Fault Using Extended Kalman Filter and Unscented Kalman Filter. *Energies* **2020**, *13*. https://doi.org/10.3390/en13112972.
109. Zhang, J.; Zhan, W.; Ehsani, M. Diagnosis and Fault-Tolerant Control of Permanent Magnet Synchronous Motors with Interturn Short-Circuit Fault. *IEEE Trans. Contr. Syst. Technol.* **2023**, *31*, 1909–1916. https://doi.org/10.1109/TCST.2023.3239426.
110. He, Q.; Pan, J.; Lyu, X. Early Performance Degradation Detecting Method for PMSM Based on Change in Frequency Domain Features of Three-Phase Stator Current. *IEEE Access* **2023**, *11*, 123361–123372. https://doi.org/10.1109/ACCESS.2023.3329933.
111. Zezula, L.; Kozovsky, M.; Blaha, P. Diagnostics of Interturn Short Circuits in PMSMs with Online Fault Indicators Estimation. *IEEE Trans. Ind. Electron.* **2024**, 1–11. https://doi.org/10.1109/TIE.2024.3363775.
112. Kang, Y.; Yao, L. Fault Isolation and Estimation for Turn-to-Turn Short Circuit in Permanent Magnet Synchronous Motor. *IEEE Trans. Instrum. Meas.* **2024**, *73*, 1–11. https://doi.org/10.1109/TIM.2024.3368480.
113. Xu, Z.; Hu, C.; Yang, F.; Kuo, S.-H.; Goh, C.-K.; Gupta, A.; Nadarajan, S. Data-Driven Inter-Turn Short Circuit Fault Detection in Induction Machines. *IEEE Access* **2017**, *5*, 25055–25068. https://doi.org/10.1109/access.2017.2764474.
114. Wang, B.; Shen, C.; Xu, K.; Zheng, T. Turn-to-turn Short Circuit of Motor Stator Fault Diagnosis in Continuous State Based on Deep Auto-encoder. *IET Electr. Power Appl.* **2019**, *13*, 1598–1606. https://doi.org/10.1049/iet-epa.2019.0101.
115. Mahmoud, M.S.; Huynh, V.K.; Senanyaka, J.S.L.; Robbersmyr, K.G. Robust Multiple-Fault Diagnosis of PMSM Drives Under Variant Operations and Noisy Conditions. *IEEE Open J. Ind. Electron. Soc.* **2023**, *4*, 762–772. https://doi.org/10.1109/OJIES.2024.3350443.
116. Maraaba, L.S.; Milhem, A.S.; Nemer, I.A.; Al-Duwaish, H.; Abido, M.A. Convolutional Neural Network-Based Inter-Turn Fault Diagnosis in LSPMSMs. *IEEE Access* **2020**, *8*, 81960–81970. https://doi.org/10.1109/access.2020.2991137.
117. Shih, K.-J.; Hsieh, M.-F.; Chen, B.-J.; Huang, S.-F. Machine Learning for Inter-Turn Short-Circuit Fault Diagnosis in Permanent Magnet Synchronous Motors. *IEEE Trans. Magn.* **2022**, *58*, 1–7. https://doi.org/10.1109/tmag.2022.3169173.
118. Song, Q.; Wang, M.; Lai, W.; Zhao, S. On Bayesian Optimization-Based Residual CNN for Estimation of Inter-Turn Short Circuit Fault in PMSM. *IEEE Trans. Power Electron.* **2023**, *38*, 2456–2468. https://doi.org/10.1109/tpel.2022.3207181.
119. Wang, M.; Song, Q.; Lai, W. On Model-Based Transfer Learning Method for the Detection of Inter-Turn Short Circuit Faults in PMSM. *Sensors* **2023**, *23*, 9145. https://doi.org/10.3390/s23229145.
120. Li, Y.; Wang, R.; Mao, R.; Zhang, Y.; Zhu, K.; Li, Y.; Zhang, J. A Fault Diagnosis Method Based on an Improved Deep Q-Network for the Interturn Short Circuits of a Permanent Magnet Synchronous Motor. *IEEE Trans. Transp. Electrific.* **2024**, *10*, 3870–3887. https://doi.org/10.1109/TTE.2023.3306437.

121. Li, H.; Shen, J.; Shi, C.; Shi, T. Hybrid Learning Model-Based Inter-Turn Short Circuit Fault Diagnosis of PMSM. In Proceedings of the 2023 IEEE Transportation Electrification Conference and Expo, Asia-Pacific (ITEC Asia-Pacific); IEEE: Chiang Mai, Thailand, November 28 2023; pp. 1–6.
122. Parvin, F.; Faiz, J.; Qi, Y.; Kalhor, A.; Akin, B. A Comprehensive Inter-Turn Fault Severity Diagnosis Method for Permanent Magnet Synchronous Motors Based on Transformer Neural Networks. *IEEE Trans. Ind. Inform.* **2023**, 1–11. https://doi.org/10.1109/tii.2023.3242773.
123. Lee, H.; Jeong, H.; Koo, G.; Ban, J.; Kim, S.W. Attention Recurrent Neural Network-Based Severity Estimation Method for Interturn Short-Circuit Fault in Permanent Magnet Synchronous Machines. *IEEE Trans. Ind. Electron.* **2021**, *68*, 3445–3453. https://doi.org/10.1109/tie.2020.2978690.
124. Tallam, R.M.; Habetler, T.G.; Harley, R.G. Stator Winding Turn-Fault Detection for Closed-Loop Induction Motor Drives. *IEEE Trans. Ind. Appl.* **2003**, *39*, 720–724. https://doi.org/10.1109/tia.2003.811784.
125. Pietrzak, P.; Wolkiewicz, M. On-Line Detection and Classification of PMSM Stator Winding Faults Based on Stator Current Symmetrical Components Analysis and the KNN Algorithm. *Electronics* **2021**, *10*. https://doi.org/10.3390/electronics10151786.
126. Zhang, J.; Wang, Y.; Zhu, K.; Zhang, Y.; Li, Y. Diagnosis of Interturn Short-Circuit Faults in Permanent Magnet Synchronous Motors Based on Few-Shot Learning under a Federated Learning Framework. *IEEE Trans. Ind. Inform.* **2021**, *17*, 8495–8504. https://doi.org/10.1109/tii.2021.3067915.
127. Haddad, R.Z.; Strangas, E.G. On the Accuracy of Fault Detection and Separation in Permanent Magnet Synchronous Machines Using MCSA/MVSA and LDA. *IEEE Trans. Energy Convers.* **2016**, *31*, 924–934. https://doi.org/10.1109/TEC.2016.2558183.
128. Maraaba, L.S.; Al-Hamouz, Z.M.; Milhem, A.S.; Abido, M.A. Neural Network-Based Diagnostic Tool for Detecting Stator Inter-Turn Faults in Line Start Permanent Magnet Synchronous Motors. *IEEE Access* **2019**, *7*, 89014–89025. https://doi.org/10.1109/access.2019.2923746.
129. Wei, D.; Liu, K.; Wang, J.; Zhou, S.; Li, K. ResNet-18 Based Inter-Turn Short Circuit Fault Diagnosis of PMSMs with Consideration of Speed and Current Loop Bandwidths. *IEEE Trans. Transp. Electrific.* **2023**, 1–1. https://doi.org/10.1109/TTE.2023.3319157.
130. Pietrzak, P.; Wolkiewicz, M.; Orlowska-Kowalska, T. PMSM Stator Winding Fault Detection and Classification Based on Bispectrum Analysis and Convolutional Neural Network. *IEEE Trans. Ind. Electron.* **2023**, *70*, 5192–5202. https://doi.org/10.1109/tie.2022.3189076.
131. Li, L.; Liao, S.; Zou, B.; Liu, J. Mechanism-Based Fault Diagnosis Deep Learning Method for Permanent Magnet Synchronous Motor. *Sensors* **2024**, *24*, 6349. https://doi.org/10.3390/s24196349.
132. Zsuga, Á.; Dineva, A. Data-Driven Onboard Inter-Turn Short Circuit Fault Diagnosis for Electric Vehicles by Using Real-Time Simulation Environment. *IEEE Access* **2023**, 1–1. https://doi.org/10.1109/ACCESS.2023.3344483.
133. Kumar, R.R.; Randazzo, V.; Cirrincione, G.; Cirrincione, M.; Pasero, E.; Tortella, A.; Andriollo, M. Induction Machine Stator Fault Tracking Using the Growing Curvilinear Component Analysis. *IEEE Access* **2021**, *9*, 2201–2212. https://doi.org/10.1109/access.2020.3047202.
134. Wu, X.; Geng, Y.; Li, M.; Wang, W.; Tu, M. Inter-Turn Short Circuit Diagnosis of Permanent Magnet Synchronous Motor Based on Siamese Convolutional Neural Network Under Small Fault Samples. *IEEE Sensors J.* **2024**, *24*, 26982–26993. https://doi.org/10.1109/JSEN.2024.3423751.
135. Chen, Z.; Liang, D.; Jia, S.; Yang, S. Model-Based Data Normalization for Data-Driven PMSM Fault Diagnosis. *IEEE Trans. Power Electron.* **2024**, *39*, 11596–11612. https://doi.org/10.1109/TPEL.2024.3398802.
136. Lv, K.; Wang, D.; Huang, W.; Hu, J. Research on Fault Indicator for Integrated Fault Diagnosis System of PMSM Based on Stator Tooth Flux. *IEEE J. Emerg. Sel. Topics Power Electron.* **2024**, *12*, 985–996. https://doi.org/10.1109/JESTPE.2023.3334866.
137. Rafiei, V.; Khoshlessan, M.; Caicedo-Narvaez, C.; Fahimi, B. Detection of Inter-Turn Short Circuit in Stator Windings of Electric Machines Using Magnetic Symmetry Index and Machine Learning Methods. *IEEE Trans. Energy Convers.* **2024**, 1–11. https://doi.org/10.1109/TEC.2024.3434395.
138. Cao, W.; Huang, R.; Wang, H.; Lu, S.; Hu, Y.; Hu, C.; Huang, X. Analysis of Inter-Turn Short-Circuit Faults in Brushless DC Motors Based on Magnetic Leakage Flux and Back Propagation Neural Network. *IEEE Trans. Energy Convers.* **2023**, *38*, 2273–2281. https://doi.org/10.1109/TEC.2023.3285899.

139. Li, H.; Shi, T. Diagnosis of Inter-Turn Short-Circuit Incipient Fault in Permanent Magnet Synchronous Motors Using Input Current on the Power Side. *IEEE Trans. Ind. Inf.* **2024**, 1–12. https://doi.org/10.1109/TII.2024.3431632.
140. Ibrahim, R.; Zemouri, R.; Kedjar, B.; Merkhouf, A.; Tahan, A.; Al-Haddad, K.; Lafleur, F. Non-Invasive Detection of Rotor Inter-Turn Short Circuit of a Hydrogenerator Using AI-Based Variational Autoencoder. *IEEE Trans. on Ind. Applicat.* **2023**, 1–10. https://doi.org/10.1109/TIA.2023.3281311.
141. Li, G.J.; Ren, B.; Zhu, Z.Q.; Foster, M.P.; Stone, D.A. Demagnetization Withstand Capability Enhancement of Surface Mounted PM Machines Using Stator Modularity. *IEEE Trans. Ind. Appl.* **2018**, *54*, 1302–1311. https://doi.org/10.1109/tia.2017.2777922.
142. Du, Y.; Wu, L.; Zhan, H.; Fang, Y. Influence of Dimensional Parameters on Three-Phase Short Circuit and Demagnetization in Surface-Mounted PM Machines. *IEEE Trans. Energy Convers.* **2021**, *36*, 2514–2523. https://doi.org/10.1109/tec.2021.3051140.
143. Urresty, J.-C.; Riba, J.-R.; Romeral, L. A Back-Emf Based Method to Detect Magnet Failures in PMSMs. *IEEE Trans. Magn.* **2013**, *49*, 591–598. https://doi.org/10.1109/tmag.2012.2207731.
144. Urresty, J.-C.; Riba, J.-R.; Delgado, M.; Romeral, L. Detection of Demagnetization Faults in Surface-Mounted Permanent Magnet Synchronous Motors by Means of the Zero-Sequence Voltage Component. *IEEE Trans. Energy Convers.* **2012**, *27*, 42–51. https://doi.org/10.1109/tec.2011.2176127.
145. Zhan, H.; Wu, L.; Lyu, Z.; Du, Y.; Fang, Y. Uneven Demagnetization Fault Diagnosis in Dual Three-Phase Permanent Magnet Machines Based on Electrical Signal Difference. *IEEE Trans. Transp. Electrif.* **2022**, 1–1. https://doi.org/10.1109/tte.2022.3217401.
146. Zafarani, M.; Goktas, T.; Akin, B.; Fedigan, S.E. An Investigation of Motor Topology Impacts on Magnet Defect Fault Signatures. *IEEE Trans. Ind. Electron.* **2017**, *64*, 32–42. https://doi.org/10.1109/tie.2016.2609380.
147. Rajagopalan, S.; Roux, W. le; Habetler, T.G.; Harley, R.G. Dynamic Eccentricity and Demagnetized Rotor Magnet Detection in Trapezoidal Flux (Brushless DC) Motors Operating under Different Load Conditions. *IEEE Trans. Power Electron.* **2007**, *22*, 2061–2069. https://doi.org/10.1109/tpel.2007.904183.
148. Garcia-Calva, T.A.; Gyftakis, K.N.; Skarmoutsos, G.A.; Mueller, M.; Morinigo-Sotelo, D.; Romero-Troncoso, R.D.J. Advanced Signal Processing Techniques for Demagnetization Detection in PM Generators at Variable Speed. *IEEE Trans. on Ind. Applicat.* **2023**, 1–10. https://doi.org/10.1109/TIA.2023.3312362.
149. Ruiz, J.R.R.; Rosero, J.A.; Espinosa, A.G.; Romeral, L. Detection of Demagnetization Faults in Permanent-Magnet Synchronous Motors under Nonstationary Conditions. *IEEE Trans. Magn.* **2009**, *45*, 2961–2969. https://doi.org/10.1109/tmag.2009.2015942.
150. Prieto, M.D.; Espinosa, A.G.; Ruiz, J.R.R.; Urresty, J.C.; Ortega, J.A. Feature Extraction of Demagnetization Faults in Permanent-Magnet Synchronous Motors Based on Box-Counting Fractal Dimension. *IEEE Trans. Ind. Electron.* **2011**, *58*, 1594–1605. https://doi.org/10.1109/tie.2010.2066538.
151. Wang, C.; Delgado Prieto, M.; Romeral, L.; Chen, Z.; Blaabjerg, F.; Liu, X. Detection of Partial Demagnetization Fault in PMSMs Operating under Nonstationary Conditions. *IEEE Trans. Magn.* **2016**, *52*, 1–4. https://doi.org/10.1109/tmag.2015.2511003.
152. Gyftakis, K.N.; Garcia-Calva, T.A.; Skarmoutsos, G.A.; Morinigo-Sotelo, D.; Mueller, M.; Romero-Troncoso, R. de J. Demagnetization Monitoring and Identification in PM Generators with Concentrated Windings during Transient Conditions. *IEEE Trans. Ind. Appl.* **2022**, 1–10. https://doi.org/10.1109/tia.2022.3221699.
153. Espinosa, A.G.; Rosero, J.A.; Cusido, J.; Romeral, L.; Ortega, J.A. Fault Detection by Means of Hilbert–Huang Transform of the Stator Current in a PMSM with Demagnetization. *IEEE Trans. Energy Convers.* **2010**, *25*, 312–318. https://doi.org/10.1109/tec.2009.2037922.
154. Chen, Z.; Liang, Z.; Liang, D.; Jia, S. Partial Demagnetization Fault Analysis and Diagnosis for Fractional Slot Concentrated Winding PMSMs Based on DQ-Axis Components. *IEEE Trans. Energy Convers.* **2024**, 1–11. https://doi.org/10.1109/TEC.2024.3505255.
155. Goktas, T.; Zafarani, M.; Akin, B. Discernment of Broken Magnet and Static Eccentricity Faults in Permanent Magnet Synchronous Motors. *IEEE Trans. Energy Convers.* **2016**, *31*, 578–587. https://doi.org/10.1109/tec.2015.2512602.
156. Zafarani, M.; Goktas, T.; Akin, B. A Comprehensive Analysis of Magnet Defect Faults in Permanent Magnet Synchronous Motors. *IEEE Trans. on Ind. Applicat.* **2015**, 1–1. https://doi.org/10.1109/TIA.2015.2487440.

157. Radwan-Pragłowska, N.; Wegiel, T. Diagnostics of Interior PM Machine Rotor Faults Based on EMF Harmonics. *Energies* **2024**, *17*, 2198. https://doi.org/10.3390/en17092198.
158. Rasid, S.A.; Gyftakis, K.N.; Mueller, M. Comparative Investigation of Three Diagnostic Methods Applied to Direct-Drive Permanent Magnet Machines Suffering from Demagnetization. *Energies* **2023**, *16*, 2767. https://doi.org/10.3390/en16062767.
159. Gritli, Y.; Rossi, C.; Rizzoli, G.; Mengoni, M.; Tani, A.; Casadei, D. Robust Online Magnet Demagnetization Diagnosis in Asymmetrical Six-Phase AC Permanent Magnet Motor Drives. *IEEE Access* **2023**, *11*, 50769–50780. https://doi.org/10.1109/ACCESS.2023.3278025.
160. Hong, J.; Park, S.; Hyun, D.; Kang, T.; Lee, S.B.; Kral, C.; Haumer, A. Detection and Classification of Rotor Demagnetization and Eccentricity Faults for PM Synchronous Motors. *IEEE Trans. on Ind. Applicat.* **2012**, *48*, 923–932. https://doi.org/10.1109/TIA.2012.2191253.
161. Jongman, H.; Doosoo, H.; Sang Bin, L.; Ji-Yoon, Y.; Kwang-Woon, L. Automated Monitoring of Magnet Quality for Permanent-Magnet Synchronous Motors at Standstill. *IEEE Trans. Ind. Appl.* **2010**, *46*, 1397–1405. https://doi.org/10.1109/tia.2010.2049811.
162. Fernandez, D.; Reigosa, D.D.; Guerrero, J.M.; Zhu, Z.-Q.; Briz, F. Permanent-Magnet Magnetization State Estimation Using High-Frequency Signal Injection. *IEEE Trans. Ind. Appl.* **2016**, *52*, 2930–2940. https://doi.org/10.1109/tia.2016.2541616.
163. Diaz Reigosa, D.; Fernandez, D.; Zhu, Z.-Q.; Briz, F. PMSM Magnetization State Estimation Based on Stator-Reflected PM Resistance Using High-Frequency Signal Injection. *IEEE Trans. Ind. Appl.* **2015**, *51*, 3800–3810. https://doi.org/10.1109/tia.2015.2437975.
164. He, W.; Hang, J.; Ding, S.; Sun, L.; Hua, W. Robust Diagnosis of Partial Demagnetization Fault in PMSMs Using Radial Air-Gap Flux Density under Complex Working Conditions. *IEEE Trans. Ind. Electron.* **2024**, 1–10. https://doi.org/10.1109/TIE.2024.3349520.
165. Zeng, C.; Huang, S.; Lei, J.; Wan, Z.; Yang, Y. Online Rotor Fault Diagnosis of Permanent Magnet Synchronous Motors Based on Stator Tooth Flux. *IEEE Trans. Ind. Appl.* **2021**, *57*, 2366–2377. https://doi.org/10.1109/tia.2021.3058541.
166. Orviz, M.; Laborda, D.F.; Reigosa, D.; Lee, H.-J.; Rafaq, M.S.; Lee, S.B.; Briz, F. Demagnetization Detection and Severity Assessment in PMSMs Using Search Coils Exploiting Machine's Symmetry. *IEEE Trans. on Ind. Applicat.* **2023**, *59*, 4021–4034. https://doi.org/10.1109/TIA.2023.3267772.
167. Im, J.-H.; Kang, J.-K.; Heo, J.-H.; Hur, J. Utilization of Multiple Planar Search Coils for Diagnosing Imbalance Irreversible Demagnetization Faults in PMSMs Along the Z-Axis. *IEEE Trans. on Ind. Applicat.* **2024**, *60*, 5988–5997. https://doi.org/10.1109/TIA.2024.3381915.
168. Huang, W.; Chen, J.; Su, W.; Liu, H.; Lv, K.; Hu, J. A Period Energy Method for Demagnetization Detection in Surface Permanent Magnet Motors with Search Coils. *Electronics* **2023**, *12*, 3514. https://doi.org/10.3390/electronics12163514.
169. Naderi, P. Magnetic-Equivalent-Circuit Approach for Inter-Turn and Demagnetisation Faults Analysis in Surface Mounted Permanent-Magnet Synchronous Machines Using Pole Specific Search-Coil Technique. *IET Electric Power Applications* **2018**, *12*, 916–928. https://doi.org/10.1049/iet-epa.2017.0403.
170. Rafaq, M.S.; Lee, H.; Park, Y.; Lee, S.-B.; Orviz Zapico, M.; Fernandez, D.; Diaz-Reigosa, D.; Briz, F. Airgap Search Coil Based Identification of PM Synchronous Motor Defects. *IEEE Trans. Ind. Electron.* **2022**, *69*, 6551–6560. https://doi.org/10.1109/tie.2021.3095810.
171. Skarmoutsos, G.A.; Gyftakis, K.N.; Mueller, M. Detecting Partial Demagnetization in AFPM Generators by Monitoring Speed and EMF Induced in a Supplemental Winding. *IEEE Trans. Ind. Inform.* **2022**, *18*, 3295–3305. https://doi.org/10.1109/tii.2021.3053993.
172. Gao, C.; Li, B.; Chen, H.; Xu, Y.; Xu, X.; Si, J.; Hu, Y. A Less-Invasive Method for Accurately Diagnosing of Demagnetization Fault in PMSM Using Rotor Partition. *IEEE Trans. Transp. Electrif.* **2022**, 1–1. https://doi.org/10.1109/tte.2022.3201156.
173. Chen, H.; Fang, C.; Dong, J.; Lu, S.; Pires, V.; Martins, J.; Aguirre, M.P. Diagnosis of Inter-Turn Short-Circuit of SRM Based on Ratio of Current Components. *IEEE Trans. Transp. Electrif.* **2022**, 1–1. https://doi.org/10.1109/tte.2022.3224596.

174. Skarmoutsos, G.A.; Gyftakis, K.N.; Mueller, M.A. A New Approach to PM Machine Fault Diagnostics Using Two Magnetically-Coupled Search-Coils.; 2022; pp. 1616–1621.
175. Jeong, J.; Lee, H.; Orviz, M.; Lee, S.B.; Reigosa, D.; Briz, F. Detection of Trailing Edge PM Demagnetization in Surface PM Synchronous Motors. *IEEE Trans. Ind. Appl.* **2023**, 1–9. https://doi.org/10.1109/tia.2023.3247402.
176. Goktas, T.; Arkan, M.; Mamis, M.S.; Akin, B. Broken Rotor Bar Fault Monitoring Based on Fluxgate Sensor Measurement of Leakage Flux. In Proceedings of the 2017 IEEE International Electric Machines and Drives Conference (IEMDC); IEEE: Miami, FL, USA, May 2017; pp. 1–6.
177. Goktas, T.; Zafarani, M.; Lee, K.W.; Akin, B.; Sculley, T. Comprehensive Analysis of Magnet Defect Fault Monitoring through Leakage Flux. *IEEE Trans. Magn.* **2017**, *53*, 1–10. https://doi.org/10.1109/tmag.2016.2617318.
178. Xu, Q.; Liu, X.; Miao, W.; Pong, P.W.T.; Liu, C. Online Detecting Magnet Defect Fault in PMSG with Magnetic Sensing. *IEEE Trans. Transp. Electrif.* **2021**, *7*, 2775–2786. https://doi.org/10.1109/tte.2021.3073630.
179. Reigosa, D.; Fernandez, D.; Park, Y.; Diez, A.B.; Lee, S.B.; Briz, F. Detection of Demagnetization in Permanent Magnet Synchronous Machines Using Hall-Effect Sensors. *IEEE Trans. Ind. Appl.* **2018**, *54*, 3338–3349. https://doi.org/10.1109/tia.2018.2810123.
180. Reigosa, D.; Fernandez, D.; Martinez, M.; Park, Y.; Lee, S.B.; Briz, F. Permanent Magnet Synchronous Machine Non-Uniform Demagnetization Detection Using Zero-Sequence Magnetic Field Density. *IEEE Trans. Ind. Appl.* **2019**, *55*, 3823–3833. https://doi.org/10.1109/tia.2019.2914892.
181. Park, Y.; Yang, C.; Lee, S.B.; Lee, D.-M.; Fernandez, D.; Reigosa, D.; Briz, F. Online Detection and Classification of Rotor and Load Defects in PMSMs Based on Hall Sensor Measurements. *IEEE Trans. Ind. Appl.* **2019**, *55*, 3803–3812. https://doi.org/10.1109/tia.2019.2911252.
182. Park, Y.; Fernandez, D.; Lee, S.B.; Hyun, D.; Jeong, M.; Kommuri, S.K.; Cho, C.; Diaz Reigosa, D.; Briz, F. Online Detection of Rotor Eccentricity and Demagnetization Faults in PMSMs Based on Hall-Effect Field Sensor Measurements. *IEEE Trans. Ind. Appl.* **2019**, *55*, 2499–2509. https://doi.org/10.1109/tia.2018.2886772.
183. Ebrahimi, B.M.; Faiz, J. Demagnetization Fault Diagnosis in Surface Mounted Permanent Magnet Synchronous Motors. *IEEE Trans. Magn.* **2013**, *49*, 1185–1192. https://doi.org/10.1109/tmag.2012.2217978.
184. Yang, C.; Wang, Y.; Qiu, H.; Chen, S.; Lian, Z. Electromagnetic Vibration of High-Voltage Line-Start Permanent Magnet Synchronous Motor with Demagnetization Fault. *J. Electr. Eng. Technol.* **2024**, *19*, 4143–4158. https://doi.org/10.1007/s42835-024-01828-5.
185. Ai, Q.; Wei, H.; Li, T.; Dou, H.; Zhao, W.; Zhang, Y. Online Demagnetization Fault Recognition for Permanent Magnet Motors Based on the Hall-Effect Analog Sampling. *IEEE Trans. Power Electron.* **2023**, *38*, 3600–3611. https://doi.org/10.1109/tpel.2022.3218954.
186. De Bisschop, J.; Abdallh, A.; Sergeant, P.; Dupre, L. Identification of Demagnetization Faults in Axial Flux Permanent Magnet Synchronous Machines Using an Inverse Problem Coupled with an Analytical Model. *IEEE Trans. Magn.* **2014**, *50*, 1–4. https://doi.org/10.1109/tmag.2014.2316851.
187. De Bisschop, J.; Vansompel, H.; Sergeant, P.; Dupre, L. Demagnetization Fault Detection in Axial Flux PM Machines by Using Sensing Coils and an Analytical Model. *IEEE Trans. Magn.* **2017**, *53*, 1–4. https://doi.org/10.1109/tmag.2017.2669480.
188. le Roux, W.; Harley, R.G.; Habetler, T.G. Detecting Rotor Faults in Low Power Permanent Magnet Synchronous Machines. *IEEE Trans. Power Electron.* **2007**, *22*, 322–328. https://doi.org/10.1109/tpel.2006.886620.
189. Moon, S.; Lee, J.; Jeong, H.; Kim, S.W. Demagnetization Fault Diagnosis of a PMSM Based on Structure Analysis of Motor Inductance. *IEEE Trans. Ind. Electron.* **2016**, *63*, 3795–3803. https://doi.org/10.1109/tie.2016.2530046.
190. Zhu, M.; Hu, W.; Kar, N.C. Torque-Ripple-Based Interior Permanent-Magnet Synchronous Machine Rotor Demagnetization Fault Detection and Current Regulation. *IEEE Trans. Ind. Appl.* **2017**, *53*, 2795–2804. https://doi.org/10.1109/tia.2016.2634518.
191. Liu, Z.; Huang, J.; Li, B. Diagnosing and Distinguishing Rotor Eccentricity from Partial Demagnetisation of Interior PMSM Based on Fluctuation of High-frequency d -axis Inductance and Rotor Flux. *IET Electr. Power Appl.* **2017**, *11*, 1265–1275. https://doi.org/10.1049/iet-epa.2016.0814.

192. Han, Y.; Chen, S.; Gong, C.; Zhao, X.; Zhang, F.; Li, Y. Accurate SM Disturbance Observer-Based Demagnetization Fault Diagnosis with Parameter Mismatch Impacts Eliminated for IPM Motors. *IEEE Trans. Power Electron.* **2023**, 1–5. https://doi.org/10.1109/tpel.2023.3245052.
193. Yi, C.-P.; Lin, Y.-J.; Ho, P.-J.; Yang, S.-C. Magnet Fault Diagnosis for Permanent Magnet Synchronous Motor Based on Flux Estimation With PWM Voltage Measurement. *IEEE Trans. Ind. Electron.* **2024**, 1–11. https://doi.org/10.1109/TIE.2024.3426031.
194. Vancini, L.; Mengoni, M.; Rizzoli, G.; Zarri, L.; Tani, A. Local Demagnetization Detection in Six-Phase Permanent Magnet Synchronous Machines. *IEEE Trans. Ind. Electron.* **2024**, *71*, 5508–5518. https://doi.org/10.1109/TIE.2023.3294603.
195. Skowron, M.; Orlowska-Kowalska, T.; Kowalski, C.T. Detection of Permanent Magnet Damage of PMSM Drive Based on Direct Analysis of the Stator Phase Currents Using Convolutional Neural Network. *IEEE Trans. Ind. Electron.* **2022**, *69*, 13665–13675. https://doi.org/10.1109/tie.2022.3146557.
196. Skowron, M. Transfer Learning-Based Fault Detection System of Permanent Magnet Synchronous Motors. *IEEE Access* **2024**, *12*, 135372–135389. https://doi.org/10.1109/ACCESS.2024.3463970.
197. Minaz, M.R.; Akcan, E. An Effective Method for Detection of Demagnetization Fault in Axial Flux Coreless PMSG with Texture-Based Analysis. *IEEE Access* **2021**, *9*, 17438–17449. https://doi.org/10.1109/access.2021.3050418.
198. Zhou, S.; Ma, C.; Ji, Z.; Feng, Q.; Zhao, Y.; Wang, Y.; Shen, Z.; Wang, D. A New Data-Driven Diagnosis Method for Compound Fault of Mixed Eccentricity and Demagnetization in External Rotor Permanent Magnet Motors. *IEEE Trans. Ind. Inf.* **2024**, *20*, 11794–11805. https://doi.org/10.1109/TII.2024.3413311.
199. Pietrzak, P.; Wolkiewicz, M. Demagnetization Fault Diagnosis of Permanent Magnet Synchronous Motors Based on Stator Current Signal Processing and Machine Learning Algorithms. *Sensors* **2023**, *23*, 1757. https://doi.org/10.3390/s23041757.
200. Koutrakos, K.; Mitronikas, E. Outlier Detection for Permanent Magnet Synchronous Motor (PMSM) Fault Detection and Severity Estimation. *Applied Sciences* **2024**, *14*, 4318. https://doi.org/10.3390/app14104318.
201. Kumar, L.; Nadarajan, S.; Vaiyapuri, V.; Gupta, A.; Soong, B.-H.; Nguyen, H.D. Decoupling of Demagnetization Characteristics to Improve the Turn-to-Turn Fault Detection in PMSM Using Machine Learning Methods. In Proceedings of the IECON 2023- 49th Annual Conference of the IEEE Industrial Electronics Society; IEEE: Singapore, Singapore, October 16 2023; pp. 1–6.
202. Du, B.; Huang, W.; Cheng, Y.; Chen, J.; Tao, R.; Cui, S. Fault Diagnosis and Separation of PMSM Rotor Faults Using Search Coil Based on MVSA and Random Forests. *IEEE Trans. Ind. Electron.* **2024**, *71*, 15089–15099. https://doi.org/10.1109/TIE.2024.3363733.
203. Kang, J.-K.; Yoo, D.-W.; Hur, J. Application and Verification of Voltage Angle-Based Fault Diagnosis Method in Six-Phase IPMSM. *IEEE Trans. on Ind. Applicat.* **2023**, 1–12. https://doi.org/10.1109/TIA.2023.3325796.
204. Meiwei, Z.; Weili, L.; Haoyue, T. Demagnetization Fault Diagnosis of the Permanent Magnet Motor for Electric Vehicles Based on Temperature Characteristic Quantity. *IEEE Trans. Transp. Electrif.* **2023**, *9*, 759–770. https://doi.org/10.1109/tte.2022.3200927.
205. Song, J.; Zhao, J.; Zhang, X.; Dong, F.; Zhao, J.; Xu, L.; Yao, Z. Accurate Demagnetization Faults Detection of Dual-Sided Permanent Magnet Linear Motor Using Enveloping and Time-Domain Energy Analysis. *IEEE Trans. Ind. Inform.* **2020**, *16*, 6334–6346. https://doi.org/10.1109/tii.2019.2962730.
206. Song, J.; Zhao, J.; Dong, F.; Zhao, J.; Xu, L.; Yao, Z. A New Demagnetization Fault Recognition and Classification Method for DPMSLM. *IEEE Trans. Ind. Inform.* **2020**, *16*, 1559–1570. https://doi.org/10.1109/tii.2019.2928008.
207. Song, J.; Liu, S.; Duan, Z.; Wu, X.; Ding, W.; Wang, X.; Lu, S. DPMSLM Demagnetization Fault Detection Based on Texture Feature Analysis of Grayscale Fusion Image. *IEEE Trans. Instrum. Meas.* **2023**, *72*, 1–12. https://doi.org/10.1109/TIM.2023.3259035.
208. Gao, C.; Gao, B.; Xu, X.; Si, J.; Hu, Y. Automatic Demagnetization Fault Location of Direct-Drive Permanent Magnet Synchronous Motor Using Knowledge Graph. *IEEE Trans. Instrum. Meas.* **2024**, *73*, 1–12. https://doi.org/10.1109/TIM.2023.3336712.

209. Huang, F.; Zhang, X.; Qin, G.; Xie, J.; Peng, J.; Huang, S.; Long, Z.; Tang, Y. Demagnetization Fault Diagnosis of Permanent Magnet Synchronous Motors Using Magnetic Leakage Signals. *IEEE Trans. Ind. Inform.* **2022**, 1–1. https://doi.org/10.1109/tii.2022.3165283.
210. Attestog, S.; Senanayaka, J.S.L.; Khang, H.V.; Robbersmyr, K.G. Robust Active Learning Multiple Fault Diagnosis of PMSM Drives with Sensorless Control under Dynamic Operations and Imbalanced Datasets. *IEEE Trans. Ind. Inform.* **2022**, 1–11. https://doi.org/10.1109/tii.2022.3227628.
211. Zhu, Z.Q.; Wu, L.J.; Mohd Jamil, M.L. Distortion of Back-EMF and Torque of PM Brushless Machines Due to Eccentricity. *IEEE Trans. Magn.* **2013**, *49*, 4927–4936. https://doi.org/10.1109/tmag.2013.2246181.
212. Dorrell, D.G.; Min-Fu Hsieh; YouGuang Guo Unbalanced Magnet Pull in Large Brushless Rare-Earth Permanent Magnet Motors With Rotor Eccentricity. *IEEE Trans. Magn.* **2009**, *45*, 4586–4589. https://doi.org/10.1109/TMAG.2009.2022338.
213. Wei, Q.; Zeng, D.; Sun, Z.; Qiu, W.; Shuai, Z.; Li, W. An Improved Conformal Mapping Method for Electromagnetic Vibration Analysis in PMSMs With Rotor Eccentricity. *IEEE Trans. Appl. Supercond.* **2024**, *34*, 1–5. https://doi.org/10.1109/TASC.2024.3425320.
214. Zhu, Z.Q.; Wu, L.J.; Mohd Jamil, M.L. Influence of Pole and Slot Number Combinations on Cogging Torque in Permanent-Magnet Machines with Static and Rotating Eccentricities. *IEEE Trans. Ind. Appl.* **2014**, *50*, 3265–3277. https://doi.org/10.1109/tia.2014.2308363.
215. Ebrahimi, B.M.; Faiz, J.; Roshtkhari, M.J. Static-, Dynamic-, and Mixed-Eccentricity Fault Diagnoses in Permanent-Magnet Synchronous Motors. *IEEE Trans. Ind. Electron.* **2009**, *56*, 4727–4739. https://doi.org/10.1109/tie.2009.2029577.
216. Rajagopalan, S.; Aller, J.M.; Restrepo, J.A.; Habetler, T.G.; Harley, R.G. Detection of Rotor Faults in Brushless DC Motors Operating Under Nonstationary Conditions. *IEEE Trans. on Ind. Applicat.* **2006**, *42*, 1464–1477. https://doi.org/10.1109/TIA.2006.882613.
217. Rajagopalan, S.; Aller, J.M.; Restrepo, J.A.; Habetler, T.G.; Harley, R.G. Analytic-Wavelet-Ridge-Based Detection of Dynamic Eccentricity in Brushless Direct Current (BLDC) Motors Functioning under Dynamic Operating Conditions. *IEEE Trans. Ind. Electron.* **2007**, *54*, 1410–1419. https://doi.org/10.1109/tie.2007.894699.
218. Rajagopalan, S.; Restrepo, J.A.; Aller, J.M.; Habetler, T.G.; Harley, R.G. Nonstationary Motor Fault Detection Using Recent Quadratic Time–Frequency Representations. *IEEE Trans. Ind. Appl.* **2008**, *44*, 735–744. https://doi.org/10.1109/tia.2008.921431.
219. Koura, M.B.; Boudinar, A.H.; Aimer, A.F.; Bendiabdellah, A.; Gherabi, Z. Diagnosis and Discernment between Eccentricity and Demagnetization Faults in PMSM Drives. *J. Power Electron.* **2021**, *21*, 563–573. https://doi.org/10.1007/s43236-020-00204-6.
220. Ebrahimi, B.M.; Faiz, J. Configuration Impacts on Eccentricity Fault Detection in Permanent Magnet Synchronous Motors. *IEEE Trans. Magn.* **2012**, *48*, 903–906. https://doi.org/10.1109/tmag.2011.2172977.
221. Jin, X.; Qiao, W.; Peng, Y.; Cheng, F.; Qu, L. Quantitative Evaluation of Wind Turbine Faults Under Variable Operational Conditions. *IEEE Trans. on Ind. Applicat.* **2016**, *52*, 2061–2069. https://doi.org/10.1109/TIA.2016.2519412.
222. Skarmoutsos, G.A.; Gyftakis, K.N.; Mueller, M. Analytical Prediction of the MCSA Signatures under Dynamic Eccentricity in PM Machines with Concentrated Non-Overlapping Windings. *IEEE Trans. Energy Convers.* **2022**, *37*, 1011–1019. https://doi.org/10.1109/tec.2021.3123662.
223. Zhan, H.; Wu, L.; Lyu, Z.; Du, Y.; Duan, R. Detecting Eccentricity Fault in Permanent Magnet Synchronous Machines by Means of Zero-Sequence Voltage Component. *IEEE Trans. on Ind. Applicat.* **2024**, *60*, 6761–6774. https://doi.org/10.1109/TIA.2024.3428468.
224. Zhou, S.; Ma, C.; Zhu, C.; Wang, J.; Gao, Y.; Wei, Y.; Liu, Z.; Feng, Q. A New Dynamic Eccentricity Diagnosis Method for Permanent Magnet Motors Considering Variable-Speed and Speed Fluctuation Conditions. *IEEE Trans. Instrum. Meas.* **2024**, 1–1. https://doi.org/10.1109/TIM.2024.3502823.
225. Hong, J.; Lee, S.B.; Kral, C.; Haumer, A. Detection of Airgap Eccentricity for Permanent Magnet Synchronous Motors Based on the D-Axis Inductance. *IEEE Trans. Power Electron.* **2012**, *27*, 2605–2612. https://doi.org/10.1109/tpel.2011.2176145.

226. Aggarwal, A.; Allafi, I.M.; Strangas, E.G.; Agapiou, J.S. Off-Line Detection of Static Eccentricity of PMSM Robust to Machine Operating Temperature and Rotor Position Misalignment Using Incremental Inductance Approach. *IEEE Trans. Transp. Electrif.* **2021**, *7*, 161–169. https://doi.org/10.1109/tte.2020.3006016.
227. Kang, K.; Song, J.; Kang, C.; Sung, S.; Jang, G. Real-Time Detection of the Dynamic Eccentricity in Permanent-Magnet Synchronous Motors by Monitoring Speed and Back EMF Induced in an Additional Winding. *IEEE Trans. Ind. Electron.* **2017**, *64*, 7191–7200. https://doi.org/10.1109/tie.2017.2686376.
228. Wang, Y.; Liu, K.; Hua, W.; Zhang, C.; Wu, Z.; Zhang, H. Analysis and Detection of Rotor Eccentricity in Permanent Magnet Synchronous Machines Based on Linear Hall Sensors. *IEEE Trans. Power Electron.* **2022**, *37*, 4719–4729. https://doi.org/10.1109/tpel.2021.3131576.
229. Ehya, H.; Nysveen, A.; Antonino-Daviu, J.A. Advanced Fault Detection of Synchronous Generators Using Stray Magnetic Field. *IEEE Trans. Ind. Electron.* **2022**, *69*, 11675–11685. https://doi.org/10.1109/tie.2021.3118363.
230. Ehya, H.; Nysveen, A.; Nilssen, R.; Liu, Y. Static and Dynamic Eccentricity Fault Diagnosis of Large Salient Pole Synchronous Generators by Means of External Magnetic Field. *IET Electric Power Applications* **2021**, *15*, 890–902. https://doi.org/10.1049/elp2.12068.
231. Cui, H.; Ma, C.; Wang, Y.; Li, X.; He, Y.; Shen, Z.; Ji, Z.; Wang, P. Analytical Calculation of Stray Magnetic Field in Interior Permanent Magnet Synchronous Motor Under Static Eccentricity Considering Nonlinear and Non-Uniform Magnetic Saturation. *IEEE Trans. Magn.* **2024**, 1–1. https://doi.org/10.1109/TMAG.2024.3504497.
232. He, Y.-L.; Zhang, Z.-J.; Tao, W.-Q.; Wang, X.-L.; Gerada, D.; Gerada, C.; Gao, P. A New External Search Coil Based Method to Detect Detailed Static Air-Gap Eccentricity Position in Nonsalient Pole Synchronous Generators. *IEEE Trans. Ind. Electron.* **2021**, *68*, 7535–7544. https://doi.org/10.1109/tie.2020.3003635.
233. Park, J.-C.; Park, S.-H.; Kim, J.-H.; Lee, S.-G.; Lee, G.-H.; Lim, M.-S. Diagnosis and Robust Design Optimization of SPMSM Considering Back EMF and Cogging Torque Due to Static Eccentricity. *Energies* **2021**, *14*, 2900. https://doi.org/10.3390/en14102900.
234. Hsieh, M.-F.; Yeh, Y.-H. Rotor Eccentricity Effect on Cogging Torque of PM Generators for Small Wind Turbines. *IEEE Trans. Magn.* **2013**, *49*, 1897–1900. https://doi.org/10.1109/TMAG.2012.2237021.
235. Chen, Z.; Wang, F.; Fan, C.; Ling, Z.; Li, Z.; Wang, Q. Analysis of Rotor Eccentricity Fault in IPMSM With Different Armature Winding Structures. *IEEE Trans. Magn.* **2023**, *59*, 1–10. https://doi.org/10.1109/TMAG.2023.3238318.
236. Du, J.; Zhong, R.; Wu, Z.; Hua, W.; Wu, Z.; Zhang, C. Effect of Eccentricity on Vibration and Noise of External-Rotor PMSM. In Proceedings of the 2024 International Conference on Electrical Machines (ICEM); IEEE: Torino, Italy, September 1 2024; pp. 1–6.
237. Conggan Ma; Shuguang Zuo Black-Box Method of Identification and Diagnosis of Abnormal Noise Sources of Permanent Magnet Synchronous Machines for Electric Vehicles. *IEEE Trans. Ind. Electron.* **2014**, *61*, 5538–5549. https://doi.org/10.1109/TIE.2014.2301767.
238. Kang, J.-K.; Hur, J. Static Eccentric Fault Diagnosis of IPMSM Using Thermocouple Sensor. In Proceedings of the 2023 IEEE Energy Conversion Congress and Exposition (ECCE); IEEE: Nashville, TN, USA, October 29 2023; pp. 4465–4468.
239. Ebrahimi, B.M.; Faiz, J.; Araabi, B.N. Pattern Identification for Eccentricity Fault Diagnosis in Permanent Magnet Synchronous Motors Using Stator Current Monitoring. *IET Electr. Power Appl.* **2010**, *4*, 418–430. https://doi.org/10.1049/iet-epa.2009.0149.
240. Ebrahimi, B.M.; Javan Roshtkhari, M.; Faiz, J.; Khatami, S.V. Advanced Eccentricity Fault Recognition in Permanent Magnet Synchronous Motors Using Stator Current Signature Analysis. *IEEE Trans. Ind. Electron.* **2014**, *61*, 2041–2052. https://doi.org/10.1109/tie.2013.2263777.
241. Sun, W.; Wang, H.; Qu, R. A Novel Data Generation and Quantitative Characterization Method of Motor Static Eccentricity with Adversarial Network. *IEEE Trans. Power Electron.* **2023**, 1–5. https://doi.org/10.1109/tpel.2023.3267883.

242. Wang, H.; Sun, W.; Jiang, D.; Liu, Z.; Qu, R. Rotor Eccentricity Quantitative Characterization Based on Physics-Informed Adversarial Network and Health Condition Data Only. *IEEE Trans. Ind. Electron.* **2024**, *71*, 6738–6752. https://doi.org/10.1109/TIE.2023.3306397.
243. Song, J.; Wu, X.; Qian, L.; Lv, W.; Wang, X.; Lu, S. PMSLM Eccentricity Fault Diagnosis Based on Deep Feature Fusion of Stray Magnetic Field Signals. *IEEE Trans. Instrum. Meas.* **2024**, *73*, 1–12. https://doi.org/10.1109/TIM.2023.3346539.